Der Anschnitt, Beih. 42, S. 143–162, 2019

Peter Tropper, Gert Goldenberg, Matthias Krismer, Daniel Bechter, Martin Steiner, Hans-Peter Viertler, Franz Vavtar

Mineral-chemical characterisation of chalcopyrites and fahlore-group minerals from selected Cu-ore deposits in the Eastern Alps

ABSTRACT: *In the interdisciplinary framework of the special research program (SFB) HiMAT "The History of Mining Activities in the Tyrol and Adjacent Areas: Impact on Environment and Human Societies" financed by the Austrian Science Fund 2007-2012), petrological and mineralogical investigations of ores from several copper mining sites in Tyrol (Schwaz-Brixlegg, Bachalm-Kelchalm-Röhrerbühel) and adjacent areas (Pfunderer Berg in South-Tyrol, Bartholomäberg-Silbertal in Vorarlberg, Mitterberg in Salzburg) have been carried out in the sub-project "Mineralogical-geochemical Characterization of Historic Mining Sites". The main goal of this sub-project was to summarize new and additional information on the mineralogical composition of the ores and on the chemical composition (major-, minor-, and trace elements) of the ore minerals, which were used as raw material for historic and prehistoric copper smelting. The results of this sub-project, which are summarised here provide a mineralogical and geochemical basis to develop i.) a better understanding of Bronze Age smelting in the Lower Inn Valley with respect to technological advances, and ii.) geochemical fingerprinting with respect to ore and artefact provenance and trade involving metallurgical artefacts in order to obtain a comprehensive overview of Bronze Age metallurgy in the Eastern Alps.*

KEYWORDS: CHALCOPYRITE, FAHLORE-GROUP MINERALS, RC HIMAT, GREYWACKE ZONE, EASTERN ALPS, SOUTHALPINE, KIECHLBERG

Introduction

Scientific background and state of research

The basis for a thorough archaeometric and archaeometallurgical investigation of historical mining districts is the comprehensive mineralogical/geological and archaeological study of all known ore deposits in the area (e.g. Bartelheim et al., 2002; Niederschlag et al., 2003; Nimis et al., 2012; Artioli et al., 2016). Data obtained through these studies can be used to perform provenance studies of the metals used for artefact production and thus trace prehistoric trade routes. For many decades, deciphering the provenance of metal artefacts from various prehistoric and historic periods has been essential for archaeologists, and has allowed gaining insight into cultural relations and trading routes as a function of space and time. A supraregional, large-scale geochemical survey of ore deposits and metal artefacts is crucial to track back metal artefacts to their ore sources (e.g. Junghans et al., 1960; Höppner et al., 2005; Nimis et al., 2012; Lutz & Pernicka, 2013; Pernicka & Lutz, 2015; Artioli et al., 2016). In combination with lead isotopes, the trace element compositions of artefacts have been used to discriminate between metals derived from different geological environments (e.g. Pernicka & Lutz, 2015; Artioli et al., 2016). In addition, mineralogical and mineral-chemical features characteristic for specific ore deposits will also be reflected in the resulting metal as shown from the Kiechlberg in the Lower Inn Valley by Krismer et al. (2012).

Geological overview

The Austroalpine basement of the Eastern Alps is typically polymetamorphic and records a sequence of four regional metamorphic events. It has been dated to the Late Devonian-Carboniferous, Permian, Cretaceous and Oligocene-Miocene, respectively (Hoinkes et al., 1999; Neubauer et al., 1999; Thöni, 1999; Oberhänsli et al., 2004; Schuster et al., 2001, 2004; Schmid et al., 2004; Cesare et al., 2010). The Late Devonian to Carboniferous imprint is related to the Variscan orogenic cycle (380-300 Ma), which resulted from the collision of the Gondwana and Laurussia continents and led to the formation of the Pangea supercontinent. In the Permian and Early

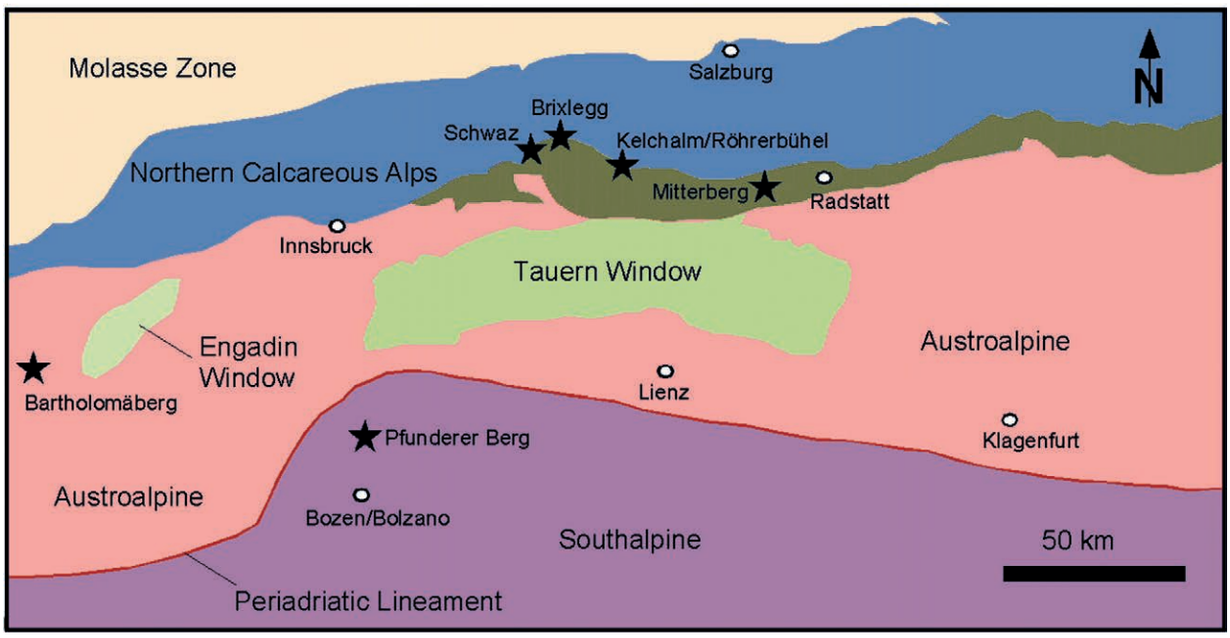

Fig. 1: Simplified tectonic overview of the Eastern Alps. Metallogenically the most important tectonic unit is the Greywacke Zone (dark greenish brown). Although this unit is part of the Austroalpine units it is shown separately in this Figure. It is bordered to the north by the sediments of the Northern Calcareous Alps (blue) and to the south by the Austroalpine (Innsbruck Quartzphyllite) and the Penninic Tauern Window (green). The Southalpine (purple) occurs to the south of the Periadriatic lineament (red line). The stars indicate the position of the ore deposits where Brixlegg also includes the Mauken ore deposits.

Triassic, large portions of the Austroalpine units were affected by lithospheric extension, due to the break-up of Pangea, and by related high-temperature/low-pressure metamorphism. The Eo-Alpine metamorphic event in the Cretaceous is related to intracontinental shortening within the northern spur of the Adriatic plate. Finally, in Oligocene to Miocene times, the continental collision between the Adriatic plate and the European plate after the closure of the Penninic oceans resulted in the Alpine orogeny and related metamorphism. The more southerly Southalpine units are separated from the Austroalpine units by the Periadriatic Lineament (Fig. 1). These units were not metamorphosed during the Alpine orogeny and consist of a Variscan metamorphic basement and a Permian-Mesozoic volcanic and sedimentary cover (Sassi & Spiess, 1993).

The Eastern Alps are known for their numerous fahl-ore- and chalcopyrite-rich copper deposits (Weber, 1997; Nimis et al., 2012; and references therein). The main mining districts are aligned along the west-east striking Northern Greywacke Zone (GWZ), which consists of Palaeozoic low-grade metamorphic schists with intercalated basic to acidic meta-vulcanites and marbles (Fig. 1). The west end of the GWZ is near the city of Schwaz in the Lower Inn Valley (Tyrol), where the largest fahlore-group mineral deposits of the Eastern Alps occur (Schwaz-Brixlegg mining district; Weber, 1997). East of Schwaz-Brixlegg, the mining districts of Röhrerbühel/Kitzbühel and Kelchalm/Jochberg contain extensive chalcopyrite deposits. At Röhrerbühel, fahlore-rich mineralizations are also known. Towards Salzburg, to the west of Bischofshofen, the Mitterberg mining district is found, which represents the largest copper (chalcopyrite) deposit of the whole Alps. Other significant copper ore districts include the chalcopyrite deposits from the Montafon (Bartholomäberg, Silbertal) in Vorarlberg, which occur in the Phyllitgneiss Zone as well as the Pfunderer Berg near Klausen in South Tyrol in the Southalpine domain. Due to their historical importance for metallurgy and metal trade in the Eastern Alps, prior to 2006 before the onset of the special research program HiMAT most geochemical, mineralogical and mining archaeological investigations so far have been focussed on the mining districts of Schwaz-Brixlegg and Mitterberg. In particular, only few mineral chemical data existed prior to this project for other important mining areas in Tyrol, Salzburg and adjacent areas, such as Vorarlberg (Montafon) and South Tyrol (cf. Brigo, 1971; Weber, 1997; Exel, 1998). In the meantime a wealth of data has been published especially with respect to the Italian ore deposits in the Southalpine domain (e.g. Nimis et al., 2012; Artioli et al., 2016).

In order to understand the beginning and the evolution of metallurgy in the Eastern Alps, a close collaboration between archaeologists, mineralogists/petrologists and geochemists is required to link the mineralogical and geochemical data of the ores from various, adjacent mining sites with the chemical data of metal artefacts from smelting and settlement sites. This is fundamental for further reconstructions concerning prehistoric mining and ancient metalworking activities. In this contribution,

we present i.) a brief description of mineral assemblages, their chemical compositions and their textures in some of the most important copper deposits investigated in the course of a Ph.D thesis (Matthias Krismer, Schwaz-Brixlegg, Pfunderer Berg) as well as three Master's theses (Daniel Bechter, Bartholomäberg-Silbertal; Martin Steiner, Kelchalm-Röhrerbühel; Hans Peter Viertler, Mitterberg), and ii.) a compilation of the major and minor element compositions of the two most important ore minerals used in alpine prehistory, namely the fahlore-group minerals and chalcopyrite.

Analytical methods

Electron-probe microanalysis

Electronprobe microanalysis (EPMA) of fahlore-group minerals and chalcopyrites was carried out using a JEOL JXA 8100 SUPERPROBE electron microprobe, equipped with five WDS detectors and a Thermo Noran EDS system, at the Institute of Mineralogy and Petrography of the University of Innsbruck. To cover the whole range of possible elements, an analysis set-up with 21 elements (S, Cu, Fe, Zn, Hg, Mn, Mo, Cd, Ni, Pb, Co, Au, Ag, Ge, In, As, Sb, Bi, Se, Sn, Te) was developed. The obtained analytic conditions were 15 kV acceleration voltage and 10 nA beam current. The counting times were 50 s for the peak and 40 s for the background. The detection limits varied between 845 ppm for Pb and 119 ppm for S. All analytical standards were pure elements, excepting for Pb (galena standard), S (troilite standard) and Hg (cinnabar standard).

The chemical composition of fahlore-group minerals and chalcopyrite

The general composition of natural fahlore-group minerals can be described by the formula $M(1)_6M(2)_6[XY_3]_4Z$ (Johnson et al., 1988) where M(1) = Cu^{1+}, Fe^{2+}, Zn^{2+}, Mn^{2+}, Hg^{2+}, Cd^{2+}; M(2) = Cu^{1+}, Ag^{1+}; X = Sb^{3+}, As^{3+}, Bi^{3+}, Te^{4+}; Y and Z = S^{2-}, Se^{2-}. The complex structure can be described by corner-sharing M(1)-Y_4 tetrahedrons (Fig. 2). Six of these tetrahedrons form a ring structure and these rings form a three-dimensional structure with large cavities occupied by the semimetals. Fahlore-group minerals show complete solid solution between the Sb (tetrahedrite) and As (tennantite) end-members. Most natural fahlore-group mineral analyses show 13 S atoms per formula unit (a.p.f.u.), although the S content can decrease below 13 a.p.f.u. Ag frequently substitutes for Cu, with a maximum of 6 a.p.f.u. of Ag (end-member freibergite), but most natural fahlore-group minerals have Ag concentrations far below 6 a.p.f.u. Fe- and Zn-rich compositions are very common in nature.

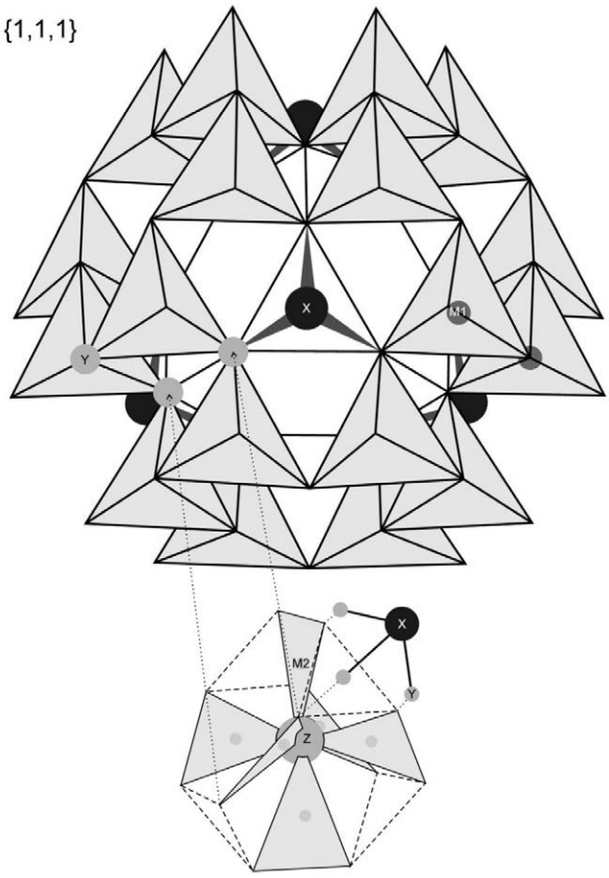

Fig. 2: Schematic illustration of the fahlore-group mineral structure according to Johnson et al. (1988). The chemical formula is $^{IV}M(1)_6{}^{III}M(2)_6[{}^{III}X\,{}^{IV}Y_3]_4{}^{VI}Z$. *M(1) = Cu, Fe, Zn, Hg; M(2) = Cu, Ag; X = As, Sb, Bi; Y = S; Z = S, Se.*

The nomenclature of fahlore-group minerals is based on the semimetal composition, the divalent metal composition and to the Cu/Ag ratio in the M(2) site. If Sb >(As + Bi + Te) the mineral is called tetrahedrite, if As >(Sb + Bi + Te) then the mineral is called tennantite. If Zn is the most frequent divalent metal atom, the fahlore-group mineral is denoted as "zincian". The same rule can be applied with other divalent cations (e.g. Fe, Cd, Hg). Any fahlore-group mineral solid solution containing $Hg/\Sigma M^{2+}$ >50% (on the atomic basis) is called "schwazite" (Mozgova et al., 1980). The name refers to a fahlore-group mineral analysis from Schwaz by Weidenbusch (1849), which reported 56% Hg end-member component (corresponding to 15.57 wt.% Hg). However, later mineral chemical investigations (e.g. Arlt & Diamond, 1998) were not able to verify any fahlore-group minerals with "schwazite" composition neither in Schwaz nor in Brixlegg. The name freibergite, indicates a mineral with dominant Sb in the X site and dominant Ag in the M(2) site.

Chalcopyrite has an ideal chemical formula $CuFeS_2$, which corresponds to 34.63 wt.% Cu, 30.43 wt.% Fe and 34.94 wt.% S, and is generally characterized by limited chemical variations.

Results

Chalcopyrite

Kelchalm-Bachalm

These deposits occur in the Jochberg Unit of the GWZ. They are closely associated with the Ordovician basic volcanism, i.e., they are pre-Alpine, and are considered to be of hydrothermal syngenetic origin (e.g. Schulz, 1997).

Petrography: The gangue consists of quartz, ankerite and dolomite and the primary ore assemblage mostly consists of chalcopyrite and pyrite (Fig. 3a). The secondary mineral assemblage mostly consists of goethite, replacing pyrite and chalcopyrite, and, subordinately, of covelline, marcasite and azurite.

Mineral chemistry: Compared to the ideal stoichiometric composition of 25 at.% Cu, 25 at.% Fe and 50 at.% S, the analyzed chalcopyrites show only slight deviations in Cu (33.93 to 35.20 at.%), Fe (28.64 to 31.19 at.%) and S (33.36 to 36.13 at.%) as shown in Table 1a. This corresponds to a formula of $Cu_{0.94\text{-}0.97}Fe_{0.95\text{-}1.02}S_{1.96\text{-}2.02}$. Most other elemental concentrations are below 1 wt.% (maximum concentrations in wt.%: Pb 0.26, Cd 0.19, Mo 0.17, In 0.17, Zn 0.16, Bi 0.11, Se 0.10). Low-temperature chalcopyrites typically show a metal to S ratio close to 1, whereas high-temperature chalcopyrites show a metal to S ratio >1 (Merwin & Lombard, 1973). Chalcopyrites from these deposits show ratios of close to 1 and can therefore be considered of low-temperature origin (Steiner, 2011) .

Pfunderer Berg

The Cu-Pb-Zn-(Ag) deposit of the Pfunderer Berg is located near the Eisack Valley to the west of Klausen in the autonomous Italian province of Alto Adige-South Tyrol. The ore deposits are situated in the rocks of the Southalpine crystalline basement. The dominant basement lithology near Klausen is the Brixen quartz phyllite, which was affected by the Variscan metamorphism and later intruded by small Permian dioritic intrusions, which led to widespread contact metamorphism. These dioritic rocks have been called klausenites (Gisser, 1926). The Pfunderer Berg ore bodies are located either in the dioritic dikes, at the contact area between the intrusive rocks and the basement rocks, or in the contact metamorphic rocks, the hornfelses. The polymetallic Pfunderer Berg deposit formed due to hydrothermal processes related to the diorite intrusions (Brigo, 1971; Exel, 1998; Fuchs, 1988; Krismer et al., 2011b). The mining district is located to the south of the SAM (Southern limit of Alpine Metamorphism, Hoinkes et al., 1999). Therefore, the ores were not affected by Alpine metamorphism however the area south of the SAM experienced at least Alpine folding and faulting (Sassi & Spiess, 1993).

Petrography: The observed complex primary sulfide assemblage consists of galena + chalcopyrite + sphalerite + freibergite-tetrahedrite solid solutions ± polybasite ± acanthite ± electrum (Fig. 3b). The most common Ag-bearing phases are freibergite-tetrahedrite solid solutions, polybasite and acanthite and occur as few microns-large, pebble-shaped inclusions in galena. In one sample, previously unreported, intimately intergrown gustavite ($AgPbBi_3S_6$) and cosalite ($Pb_2Bi_2S_5$) were found. In this case sphalerite inclusions in chalcopyrite were interpreted as exsolutions from a higher-temperature Zn-bearing high-temperature ISS (intermediate Cu-Fe-S solid solution) phase. The occurrence of α-β transformation twin lamellae in chalcopyrite indicates high temperatures of formation >500°C, consistent with a strict genetic link with the Permian magmatic activity. Old mining records frequently mention high silver contents in the ores of this deposit and galena was considered to be the dominant silver carrier. It was recently shown that the presence of abundant Ag-rich mineral inclusions is responsible for the high Ag concentrations of bulk galena (Krismer et al., 2011b).

Mineral chemistry: The highest Zn concentration of matrix chalcopyrite is only 1.55 wt.%. Similar concentrations of around 1 wt.% were reported from experiments between 400°C and 500°C in the chalcopyrite stability field (Lusk & Calder, 2004) Significant detected trace elements in chalcopyrite are Pb, Sn, and Cd. In some cases, In concentrations of up to 0.11 wt.% were measured. EPMA spot analyses of matrix chalcopyrite grains yielded no Sn contents. Only some chalcopyrite inclusions in sphalerite show up to 4.5 wt.% Sn. The solubility of stannite in chalcopyrite is high, even if only the α-chalcopyrite solid solution or the Sn-bearing intermediate solid solution (ISS) above ~470°C is capable of elevated Sn concentrations (Moh, 1975). The trace elements Pb and Cd show no preferential behaviour for either the inclusions or the large chalcopyrite grains. The Pb content ranges from below the detection limit up to 0.30 wt.% and Cd is even lower, with concentrations ranging from below the detection limit up to 0.22 wt.%. Representative analyses are given in Table 1a.

Mitterberg

The Mitterberg mining district is situated ca. 50 km south of Salzburg, between Bischofshofen and Mühlbach at the Hochkönig. Geologically, the Cu-mining district Mitterberg - Mühlbach - Larzenbach is located in the Western Greywacke Zone. The dominant host-rocks are the Pinzgau Phyllites of the Jochberg Unit. These syngenetic Cu deposits (Early Paleozoic) were remobilized during the Cretaceous, which led to the formation of an economically important ore body occurring as a large epigenetic vein. These deposits represent the largest Cu resources of the Eastern Alps (Ebner & Weber, 1997).

Petrography: This deposit consists of hydrothermal veins showing the assemblage pyrite + chalcopyrite ± fahl-

	Pfunderer Berg			Kelchalm			Mitterberg		
As	n.d.	n.d.	n.d.	n.d.	n.d.	n.d.	n.d.	0.04	0.03
S	35.79	35.60	34.78	35.06	35.85	35.35	34.05	35.38	33.36
Ag	0.02	0.01	0.02	n.d.	0.02	n.d.	n.d.	n.d.	n.d.
Cu	33.72	33.67	33.60	34.51	34.49	34.47	34.97	33.12	34.30
Ni	n.d.	0.04	n.d.	n.d.	n.d.	n.d.	n.d.	0.01	0.02
Ge	0.04	0.01	n.d.	n.d.	n.d.	0.03	0.14	n.d.	0.16
Pb	0.04	0.09	0.10	0.11	0.17	0.01	0.06	0.07	0.06
Sn	n.d.	n.d.	n.d.	n.d.	n.d.	n.d.	0.21	n.d.	0.14
Fe	30.21	29.90	30.30	30.72	30.63	30.53	30.77	30.71	31.19
Zn	0.43	0.10	0.23	0.06	0.09	0.05	0.03	0.05	0.03
Se	0.01	n.d.	0.04	0.08	n.d.	n.d.	0.01	0.01	0.05
Sb	n.d.	n.d.	0.04	0.02	n.d.	0.08	0.08	0.10	n.d.
In	0.01	0.08	0.10	0.12	0.08	0.05	0.08	0.04	0.09
Co	n.d.	0.02	n.d.	0.02	n.d.	n.d.	0.05	0.01	0.02
Te	n.d.	n.d.	n.d.	n.d.	n.d.	0.03	n.d.	n.d.	n.d.
Au	0.04	n.d.	0.06	0.14	n.d.	n.d.	n.d.	n.d.	n.d.
Cd	0.01	0.03	n.d.	0.07	n.d.	0.04	0.03	0.04	0.10
Bi	0.01	0.03	n.d.	0.02	0.04	0.04	n.d.	n.d.	0.08
Hg	0.01	0.06	0.03	n.d.	n.d.	0.03	n.d.	n.d.	n.d.
Mo	0.10	0.02	0.10	n.d.	0.08	n.d.	n.d.	0.01	n.d.
Mn	n.d.	n.d.	n.d.	n.d.	n.d.	n.d.	n.d.	n.d.	n.d.
∑ wt%	100.43	99.68	99.39	100.93	101.44	100.72	100.48	99.59	99.62
As	n.d.	n.d.	n.d.	n.d.	n.d.	n.d.	n.d.	0.001	0.001
S	2.000	2.000	2.000	2.000	2.000	2.000	2.000	2.000	2.000
Ag	<0.001	<0.001	<0.001	n.d.	<0.001	n.d.	n.d.	n.d.	n.d.
Cu	0.950	0.952	0.973	0.992	0.969	0.982	1.035	0.943	1.036
Ni	n.d.	0.001	n.d.	n.d.	n.d.	n.d.	n.d.	<0.001	<0.001
Ge	<0.001	<0.001	n.d.	n.d.	n.d.	0.001	0.004	n.d.	0.004
Pb	<0.001	<0.001	0.001	0.001	0.001	<0.001	0.001	0.001	0.001
Sn	n.d.	n.d.	n.d.	n.d.	n.d.	n.d.	0.003	n.d.	0.002
Fe	0.968	0.962	0.999	1.000	0.979	0.989	1.036	0.995	1.072
Zn	0.012	0.001	0.006	0.002	0.003	0.001	0.001	0.001	0.001
Se	<0.001	n.d.	0.001	0.002	n.d.	n.d.	<0.001	<0.001	0.001
Sb	n.d.	n.d.	0.001	<0.001	n.d.	0.001	0.001	0.002	n.d.
In	<0.001	0.001	0.002	0.002	0.001	0.001	0.001	0.001	0.002
Co	n.d.	<0.001	n.d.	0.001	n.d.	n.d.	0.001	<0.001	0.001
Te	n.d.	n.d.	n.d.	n.d.	n.d.	<0.001	n.d.	n.d.	n.d.
Au	<0.001	n.d.	0.001	0.001	n.d.	n.d.	n.d.	n.d.	n.d.
Cd	<0.001	<0.001	n.d.	0.001	n.d.	0.001	<0.001	0.001	0.002
Bi	<0.001	<0.001	n.d.	<0.001	<0.001	<0.001	n.d.	n.d.	0.001
Hg	<0.001	<0.001	<0.001	n.d.	n.d.	<0.001	n.d.	n.d.	n.d.
Mo	0.001	<0.001	0.002	n.d.	0.001	n.d.	n.d.	0.001	n.d.
Mn	n.d.	n.d.	n.d.	n.d.	n.d.	n.d.	n.d.	n.d.	n.d.
M:S	0.97	0.96	0.99	1.00	0.98	0.99	1.04	0.97	1.06

Chalcopyrite formulae calculated on the basis of 2 S. n.d.: not detected.

Tab. 1a: Representative electron-probe microanalyses of chalcopyrites

	Bartholomäberg			Mauken		
As	n.d.	0.18	0.02	n.d.	0.20	n.d.
S	35.24	35.39	35.44	34.57	34.24	36.13
Ag	n.d.	n.d.	0.01	n.d.	0.01	0.02
Cu	34.57	34.31	34.31	33.93	35.20	34.75
Ni	n.d.	0.61	n.d.	n.d.	n.d.	0.02
Ge	n.d.	n.d.	n.d.	n.d.	n.d.	n.d.
Pb	n.d.	0.14	0.10	0.08	n.d.	0.11
Sn	n.d.	n.d.	n.d.	n.d.	n.d.	n.d.
Fe	30.41	29.80	29.87	29.50	28.64	30.09
Zn	0.02	0.16	0.11	0.12	0.44	0.15
Se	0.04	0.01	n.d.	0.06	n.d.	0.01
Sb	0.04	0.03	0.03	n.d.	0.22	0.07
In	0.03	0.03	0.06	n.d.	0.02	n.d.
Co	n.d.	0.06	n.d.	n.d.	n.d.	n.d.
Te	n.d.	0.06	n.d.	n.d.	0.03	n.d.
Au	n.d.	n.d.	0.01	n.d.	n.d.	0.01
Cd	0.07	0.01	0.02	n.d.	n.d.	0.01
Bi	0.03	0.05	0.01	0.07	0.06	0.01
Hg	n.d.	n.d.	0.04	n.d.	n.d.	0.07
Mo	0.07	n.d.	0.17	n.d.	0.03	n.d.
Mn	n.d.	n.d.	n.d.	0.03	n.d.	0.02
∑ wt%	100.78	100.59	100.93	98.36	99.08	101.48
As	n.d.	0.004	<0.001	n.d.	0.005	n.d.
S	2.000	2.000	2.000	2.000	2.000	2.000
Ag	n.d.	n.d.	<0.001	n.d.	<0.001	<0.001
Cu	0.988	0.977	0.975	0.989	1.036	0.969
Ni	n.d.	0.019	n.d.	n.d.	n.d.	0.001
Ge	n.d.	n.d.	n.d.	n.d.	n.d.	n.d.
Pb	n.d.	0.001	0.001	0.001	n.d.	0.001
Sn	n.d.	n.d.	n.d.	n.d.	n.d.	n.d.
Fe	0.989	0.965	0.966	0.978	0.959	0.955
Zn	0.001	0.004	0.003	0.003	0.012	0.004
Se	0.001	<0.001	n.d.	0.001	n.d.	<0.001
Sb	0.001	0.001	<0.001	n.d.	0.003	0.001
In	<0.001	<0.001	0.001	n.d.	<0.001	n.d.
Co	n.d.	0.002	n.d.	n.d.	n.d.	n.d.
Te	n.d.	0.001	n.d.	n.d.	<0.001	n.d.
Au	n.d.	n.d.	<0.001	n.d.	n.d.	<0.001
Cd	0.001	<0.001	<0.001	n.d.	n.d.	<0.001
Bi	<0.001	<0.001	<0.001	0.001	0.001	n.d.
Hg	n.d.	n.d.	0.001	<0.001	<0.001	0.001
Mo	0.001	n.d.	0.002	n.d.	0.001	n.d.
Mn	n.d.	n.d.	n.d.	0.001	n.d.	0.001
M:S	0.99	0.98	0.97	0.99	1.00	0.97

Chalcopyrite formulae calculated on the basis of 2 S. n.d.: not detected.

Tab. 1b: Representative electron-probe microanalyses of chalcopyrites

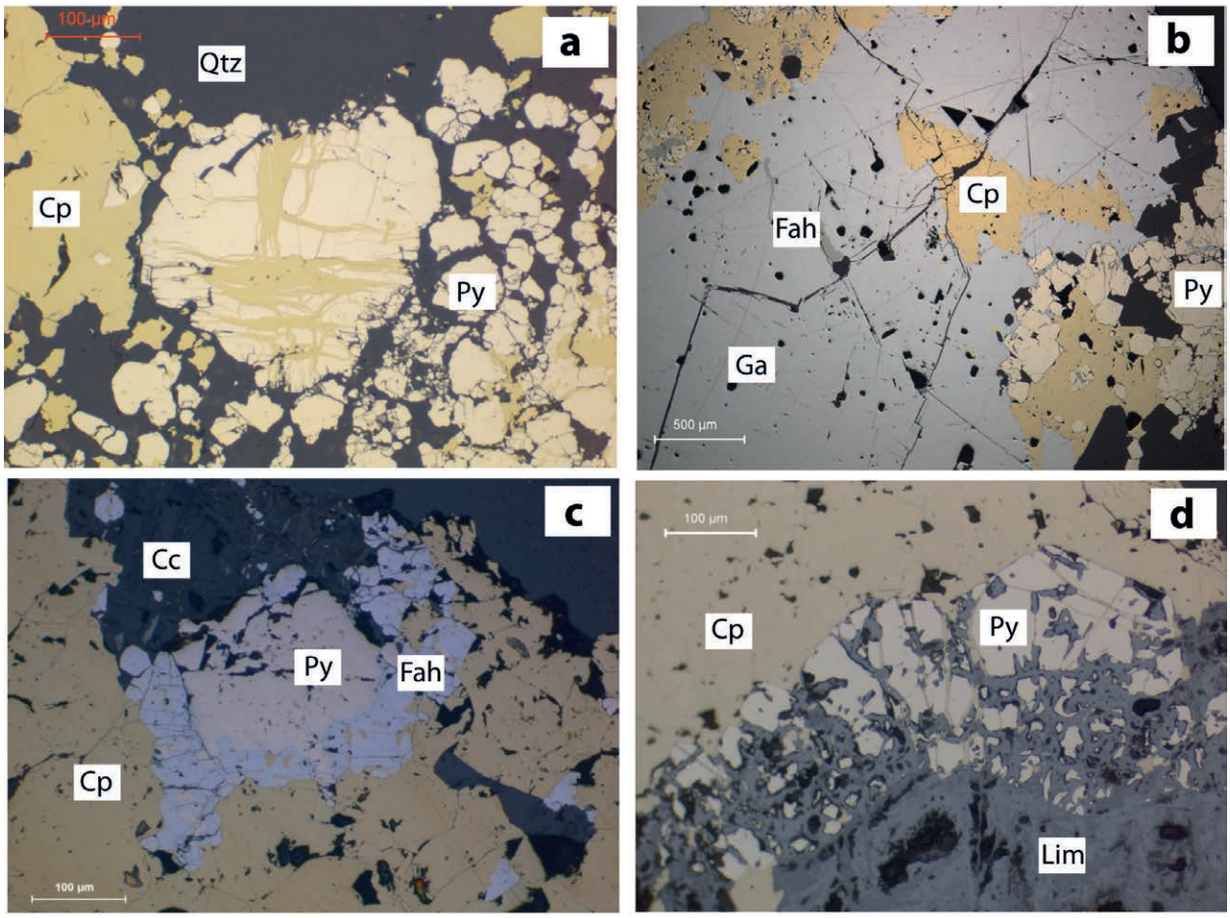

Fig. 3: Microphotograph of samples from chalcopyrite deposits. (a) Kelchalm-Bachalm; (b) Pfunderer Berg; (c) Mitterberg; (d) Bartholomäberg. The abbreviations are: Cp: chalcopyrite, Py: pyrite, Qtz: quartz, Ga: galena, Fah: fahlore-group minerals, Cc: calcite, Lim: limonite.

ore-group mineral ± gersdorffite ± sphalerite ± electrum ± corynite (Fig. 3c). The gangue consists of quartz, barite, Fe-rich carbonates (ankerite, siderite) and, rarely, wulfenite. Chalcopyrite replaces primary pyrite and gersdorffite. Chalcopyrite and pyrite were subsequently overgrown by fahlore-group minerals. Pyrite, gersdorffite, fahlore-group mineral and electrum show chemical zoning, indicating several stages of mineral growth during Eo-Alpine low-temperature remobilisation. Siderite-ankerite thermometry yielded low temperatures of formation of 190-330°C (Viertler, 2011).

Mineral chemistry: Most of the chalcopyrite analyses from Mitterberg show almost stoichiometric compositions. The mean concentrations of Cu, Fe and S are 24.40 at.%, 24.93 at.% and 50.16 at.%, respectively. In addition small amounts of As, Ni, Ge, Sn, Zn, Se were detected (Table 1a).

Bartholomäberg-Silbertal (Montafon)

The geological frame of the Montafon area is dominated by two major Austroalpine units, namely, the weakly metamorphic Northern Calcareous Alps in the northern part and the amphibolite-facies Silvretta Crystalline Complex with the Phyllitgneis Zone to the south (Oberhauser et al.,1998). The Phyllitgneis Zone is located between these major units and represents the lower metamorphic portion of the Silvretta Crystalline Complex. Regarding the genesis of the Bartholomäberg-Silbertal ore deposits Haditsch and Mostler (1986) considered it as an early possibly syndiagenetic (Permian) disseminated hydrothermal mineralization in sandstones (now quartzites) with subsequent Alpine hydrothermal remobilization. The ore deposits were exploited at two major mining sites, which are located above the village of Bartholomäberg and at the ridge above the village of Kristberg, respectively. The ore bodies occur mostly at the contact between the lower Triassic Alpine Buntsandstein (sandstones) of the Northern Calcareous Alps and the Phyllitgneis Zone. The ore bodies occur as lenses and, occasionally, as veins.

Petrography: The complex main ore paragenesis consists of chalcopyrite + fahlore-group minerals + gersdorffite + galena + sphalerite + pyrrhotite + pyrite + arsenopyrite ± corynite Ni(As,Sb)S ± alloclasite (Co,Fe)AsS (Fig. 3d). In minor concentrations acanthite Ag_2S, aikinite $PbBiCuS_3$,

paraschachnerite Ag_2Hg_3 as well as native elements like bismuth and gold occur. The gangue is mainly composed of calcite, siderite, ankerite, barite and quartz. Azurite, malachite, covellite and limonite are the main representatives of secondary minerals. Whole-rock analysis of ore and slag samples yielded high Bi contents up to 1 wt.%, which distinguishes it from the other deposits investigated so far. Fluid inclusion studies support a relatively low-temperature origin of this deposit at ca. 250-300°C (Bechter, 2009).

Mineral chemistry: The chemical composition of chalcopyrite is close to ideal, with average contents of 50.31 at.% S, 24.62 at.% Cu and 24.77 at.% Fe (Table 1b). Except for Zn (0.05 at.% Zn), no minor elements were detected in substantial concentrations.

Fahlore-group minerals

Schwaz-Brixlegg
(ore deposits in the Graywacke Zone)

The Northern Greywacke Zone consists of Ordovician to upper Carboniferous metasedimentary rocks, such as quartzphyllites, schists, marbles and basic to acidic metavolcanic rocks (Mostler, 1970). During the Variscan and Eo-Alpine orogenies, the rocks underwent greenschist-facies metamorphism and a strong tectonic overprint (Piber, 2005; Panwitz, 2006). The lithological sequence in the region of Schwaz and Brixlegg is characterized by quartzphyllites, called the Wildschönau schists and interpreted to represent a passive continental margin setting with turbidite deposits (Heinisch, 1988; Ebner & Weber, 1997; Panwitz, 2006). Pillow lavas, gabbroic rocks and metatuffites are intercalated within the Wildschönau schists. The gabbroic rocks yield Early- to Middle Ordovician ages (Panwitz, 2006). Furthermore, abundant are Devonian platform carbonates, the so-called Schwaz Dolomite. To the west of the city of Schwaz, the Kellerjochgneiss, also known as the Schwaz Augengneiss, occurs and represents a shallow granitic intrusion into the Wildschönau schists (Piber, 2005). The ore bodies of the Schwaz-Brixlegg region are mainly hosted in the Devonian Schwaz Dolomite, but they may also occur in the underlying Wildschönau Schists and as remobilizations in the overlying Northern Calcareous Alps (Goldenberg & Rieser, 2004). The ore genesis is still disputed. In earlier studies (Schulz, 1972; Gstrein, 1979), a syngenetic-sedimentary genesis was favoured. More recent studies (Frimmel & Papesch, 1990; Frimmel, 1991) suggested an epigenetic-hydrothermal origin. Arlt and Diamond (1998) carried out a detailed EPMA study of the fahlore-group minerals from the localities of Schwaz and Brixlegg. Their study provided the first comprehensive microprobe data for fahlore-group minerals from Schwaz and Brixlegg, but included only nine elements: Cu, Ag, Fe, Zn, Hg, Mn, Sb, As and S. The previously postulated geographic compositional trends, as well as the alleged occurrence of the mineral schwazite (one or more a.p.f.u. Hg in fahlore-group minerals), were refuted by their mineral chemical study. Recent comprehensive electron-probe microanalyses from Schwaz were obtained by Kharbish et al. (2007) and Krismer et al. (2011a).

Petrography: The ores of Schwaz consist of monomineralic fahlore-group mineral solid solutions (Fig. 4a). Strong compositional zoning is visible in the reflected light microscope, but more evident in BSE images. The zoning occurs along grain boundaries as well as along fractures or as irregular intergranular patterns. Late fahlore along grain boundaries and fractures appears darker in BSE images. In cases of irregularly zoned patterns within grains, the relative chronology of the different fahlore-group mineral generations is unclear since several possible miscibility gaps exist (Sack, 2017). In contrast to Schwaz, ores from Brixlegg show a more complex mineral assemblage (Fig. 4b). The main assemblage consists of large monomimeralic fahlore-group mineral grains that enclose small-scale mineral reaction domains. Similar to samples from Schwaz, the fahlore-group minerals show complex zoning patterns, nicely visible in BSE images. Three different mineral assemblages were observed in these reaction domains. Type 1 consists of enargite/luzonite-famatinite + sphalerite + pyrite + stibnite + chalcostibite. Type 2 consists of fahlore-group mineral (second generation) + enargite/luzonite-famatinite + sphalerite + pyrite + stibnite + chalcostibite. Type 3 is composed of fahlore-group mineral (second generation) + sphalerite + pyrite + stibnite + chalcostibite.

Mineral chemistry: The copper deposits of Schwaz-Brixlegg in the GWZ are characterized by more or less monomineralic fahlore-group minerals (Arlt and Diamond, 1998; Krismer et al., 2011a). The ore bodies occur as discordant veins, strata-bound bodies and breccias in the Devonian Dolomites (Schwaz Dolomite). Despite the similar age and conditions of formation, fahlore-group minerals from Schwaz and Brixlegg can be distinguished by their mineralogical and chemical compositions as shown below.

Mineral chemistry Schwaz: A total of 266 electron-probe microanalyses were made to characterize the compositional variations and zoning of fahlore-group minerals from Schwaz. The overall compositions are dominated by Cu, S, As and Sb, and include minor Fe, Zn, Hg and Ag (Tab. 2a). The mean overall mole fraction of the tetrahedrite component in fahlore-group minerals from Schwaz is 0.6 (Sb_{mean} = 18.15 wt.%) with a range between 0.4 and 0.9. The tennantite component ranges between 0.1 and 0.6 with a mean value of 0.4 (As_{mean} = 7.45 wt.%). All other possible elements substituting for Sb or As occur only as traces near or below the detection limit. Some spot analyses yielded Bi and In contents of up to 0.1 and 0.08 wt.% respectively. The Ag content is generally low and the molar fraction of the freibergite (Ag) component ranges between 0.004 and 0.020, with a mean value of 0.01 (Ag_{mean} = 0.51 wt.%). The most abundant divalent cations

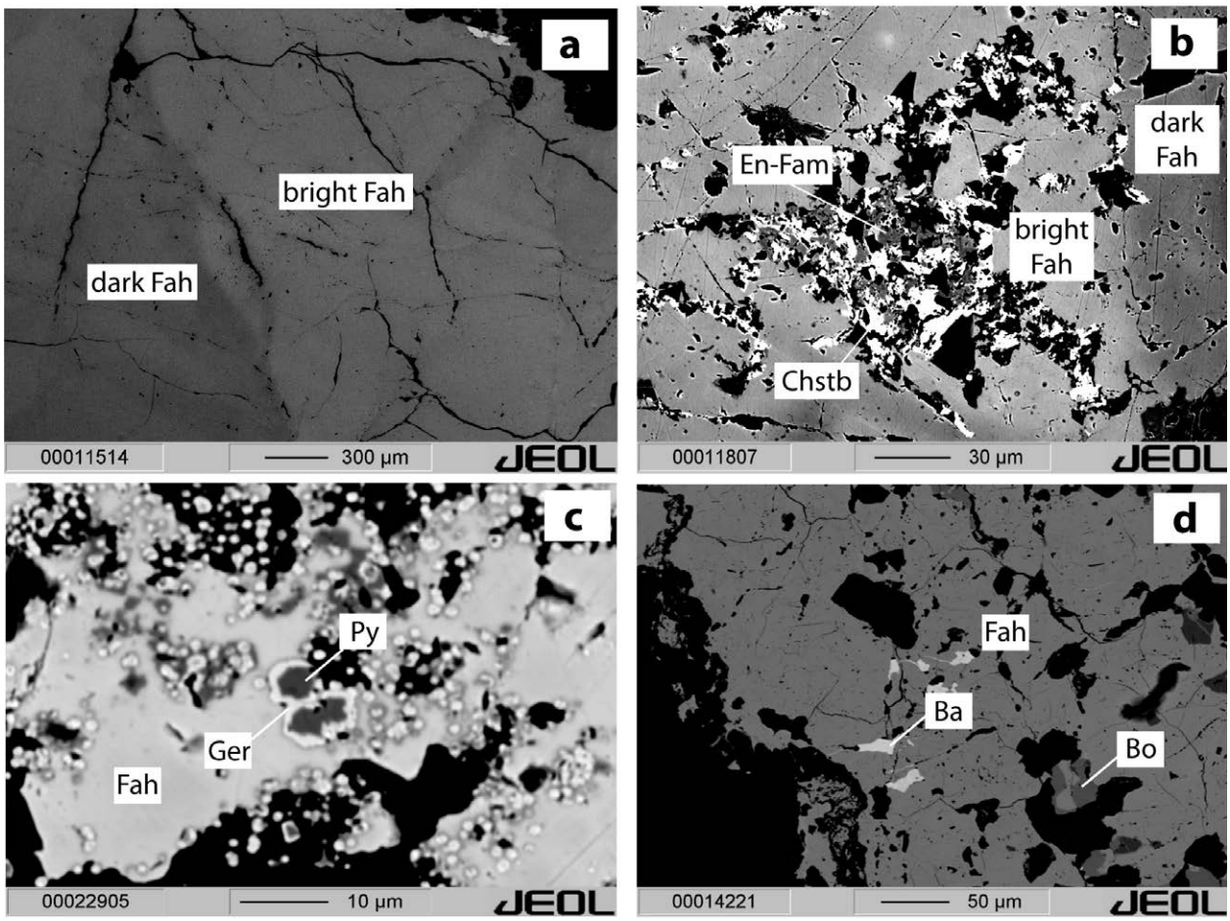

Fig. 4: Backscatter electron (BSE) images of samples from fahlore-group mineral ore deposits. (a) Schwaz; (b) Brixlegg; (c) Mauken; (d) Röhrerbühel. The abbreviations are: Fah: fahlore-group minerals, En-Fam: enargite-famatinite solid solutions, Chstb: chalcostibite, Py: pyrite, Ger: gersdorffite; Ba: balkanite; Bo: bornite.

are Fe and Zn, followed by Hg, with all other metals near or below the detection limit. Only some spot analyses revealed Sn and Cd contents near 0.5 wt.%. The mean molar fraction of the Fe component is 0.52 (Fe_{mean} = 3.09 wt.%), the mean Zn component is 0.37 (Zn_{mean} = 2.65 wt.%) and the mean Hg mole fraction is 0.09 (corresponding to 1.93 wt.% Hg). The BSE zoning of fahlore-group minerals is mainly a function of the As-Sb exchange, the higher the Sb concentration the brighter the patches appear in the image. The Hg and Ag concentrations show a correlation with the brightness. The Fe and Zn concentrations do not show a clear correlation with brightness and thus no correlation between divalent metals and semimetals can be observed. Representative fahlore-group mineral analyses from Schwaz are listed in Table 2a.

Mineral chemistry Brixlegg: The Sb and As contents in Brixlegg fahlore-group minerals are fairly similar to those at Schwaz (Table 2a). The Sb component has a mean mole fraction of 0.55 (Sb_{mean} = 16.69 wt.%) and ranges between 0.41 and 0.67. The As component has a mean mole fraction of 0.45 (As_{mean} = 8.50 wt.%) and ranges between 0.33 and 0.58. Bismuth, Indium and Germanium are occasionally above the detection limits, with up to 0.36 wt.% Bi. In is present in similar concentrations up to 0.19 wt.%. The Ge concentrations are lower, with maximum values of only 0.05 wt.%. The Ag contents are comparable to those at Schwaz and the mean molar fraction of the Ag component is 0.01 (Ag_{mean} = 0.39 wt.%). The most common divalent cations are, again, Zn and Fe, but the Hg concentration is distinctly lower compared to analyses from Schwaz. Noticeable are the high Zn contents (up to 7.61 wt.%), corresponding to a molar fraction of Zn component up to 0.92, representing nearly the Zn end-member. The mean molar fraction of the Zn component is 0.64 (Zn_{mean} = 4.96 wt.%) the mean Fe component is 0.31 (Fe_{mean} = 1.99 wt%) and the mean Hg component is 0.03 (corresponding to 0.74 wt.%). Representative fahlore-group mineral analyses from Schwaz are listed in Table 2a.

Brixlegg-Mauken
(ore deposits in the Schwaz Triassic)

The Pb-Zn-fahlore-group mineral district of the "Anis-North Tyrolean Calcareous Alps" is an east-west striking ore belt extending north of the Inn Valley from the Mieminger Kette

to the Innsbruck Nordkette (Schulz and Schroll, 1997). Thirty kilometres eastwards of the Innsbruck Nordkette, on the south side of the Inn Valley, the Schwaz Triassic (ST) contains similar ores in the same stratigraphic level (Schulz and Schroll, 1997). While the ores of the Mieminger Kette and of the Innsbruck Nordkette are mostly Pb-Zn dominated, with minor amounts of tennantite-rich fahl-ore-group minerals, the ores of the ST are dominated by tennantite-rich fahlore-group minerals and Pb-Zn phases represent only minor constituents. The copper deposits of the ST described in this study are situated south of the towns of Radfeld and Brixlegg. The landscape of this area is dominated by the Mauken Valley, which is a small N-S running tributary creek of the Inn Valley. In the following description, we will call this mining district "Mauken Area". The host rocks mainly consist of Anisian to Carnian/Norian limestones, dolomites, cellular dolomites and breccias of the Northern Calcareous Alps. In the Mauken Area, mining sites occur at Maukenötz, Silberberg and Geyer, which represent the easternmost part of the prehistoric and historic silver and copper mining area of Schwaz-Brixlegg.

Petrography: The mining districts in the Mauken Area are characterized by two ore types, which occur in two different geological units: 1.) the more common ore type consists of more or less monomineralic Fe-Zn-(Hg) tetrahedrite-tennantite and occurs in the Devonian Schwaz Dolomite which is part of the GWZ; 2.) the second ore type is hosted in the Anisian carbonates of the ST. The latter ore type shows a complex mineralogy, with tennantite-rich fahlore-group minerals (in part Ag-rich) as main copper mineral. The mineral assemblage consists of Fe-Zn tennantite + pyrite/bravoite + enargite/luzonite-famatinite ± chalcopyrite ± thiospinel ± gersdorffite-cobaltite-arsenopyrite ± galena ± sphalerite ± marcasite ± pearceite ± barite (Fig. 4c). The mineralogical and chemical composition of these ores is highly variable at a local scale (Table 2a).

Mineral chemistry: Table 2a presents selected analyses of fahlore-group minerals from the ST. The Sb and As mole fractions are the major distinguishing features between fahlore-group minerals from the GWZ and the ST. The Sb/As ratio in the GWZ is >1, whereas in the ST it is <<1. Fahlore-group minerals from the GWZ are richer in Zn, Hg and Ag and poorer in Bi compared to the ST. Analyses of GWZ samples show Bi concentrations, which are commonly above the detection limit, but in general <<0.5 wt.%. In contrast, Bi concentrations in samples from Silberberg-Geyer (ST) are below the detection limit, but some samples from Maukenötz (ST) contain Bi-rich tennantite containing >2 wt.% Bi. The Zn and Fe components of ST fahlore-group minerals show a bimodal distribution and wide scattering, ranging from near Fe end-members to near Zn end-members. Silver concentrations in both the GWZ and ST ores are generally low. Although the GWZ fahlore-group minerals are slightly richer in Ag, the mean concentration is only 0.21 wt.%, which is distinctly lower compared to the analyses of the GWZ fahlore-group mineral occurrences from the whole Schwaz and Brixlegg mining areas, as reported by Arlt and Diamond (1998) and Krismer et al. (2011a).

Röhrerbühel

The Cu ore deposit Röhrerbühel near Kitzbühel occurs in the western portion of the GWZ. The mining district is hosted in Early Paleozoic (Ordovician to Devonian) rocks, which consist of the Wildschönau Schists, basic metavolcanics, metatuffites and dolomites. Abundant Cu±Ag-bearing ore bodies occur within these Early Paleozoic metasediments containing the ore minerals chalcopyrite, pyrite, pyrrhotite and fahlore-group minerals. In the Devonian dolomites fahlore-group minerals and chalcopyrite occur. Well-known historical mining sites in the GWZ are Götschen (Brixen i. Thale), Brunnalm (Kirchberg), Röhrerbühel (Oberndorf), Sinnwell (Kitzbühel), Schattberg (Kitzbühel), Kelchalpe (Jochberg) and Kupferplatte (Jochberg). At some of these sites evidence for prehistoric mining has been documented (Mutschlechner, 1968; Goldenberg, 2004).

Petrography: Petrography revealed that the primary ore assemblage is chalcopyrite + Fe tetrahedrite + pyrite + bornite (Fig. 4d). As secondary minerals idaite, linneite, millerite, covelline, malachite, azurite, and rare Ag-bearing minerals namely pyrargyrite, an additional Ag-bearing sulfide and an amalgam-group mineral (eugenite) occur. Mineralogical investigations of the Cu deposit of Röhrerbühel also revealed the occurrence of the extremely rare Cu-Ag sulfide balkanite, $Cu_9Ag_5HgS_8$, (Steiner et al., 2010).

Mineral chemistry: Electron-probe microanalysis revealed that the fahlore-group minerals are compositionally highly variable and richer in Sb than As and thus belong to the tetrahedrite series (Table 2b). The tetrahedrite component (X_{Sb}) ranges between 0.60 and 0.90. The tennantite component (X_{As}) therefore ranges between 0.10 and 0.40, which corresponds to 2.13-7.62 wt.% As. The Fe-tetrahedrite component was calculated by the equation X_{Fe} = Fe/(Fe + Zn + Hg + Cd + Mo + Co + Sn + Pb + Ni) and ranges from 75 to 84%. The Zn-tetrahedrite component is definitely lower, ranging from 14 to 23%. All other possible elements (Te, Bi, In, Ge) substituting for Sb or As occur only as traces near or below the detection limit. The Ag content of Fe-tetrahedrite is as high as 1.54 wt.%; this corresponds to 0.24 a.p.f.u. Pb and Sn were detected only in trace concentrations. The Sn and Pb concentrations are very similar and their concentrations do not exceed 0.10-0.15 wt.%.

Pfunderer Berg

Analyses of fahlore inclusions in galena indicate compositions near the freibergite end-member. The Ag content of the inclusions is as high as 5.67 a.p.f.u. (30.3 wt.% Ag),

	Schwaz			Brixlegg			Mauken		
As	7.27	6.19	8.36	6.27	9.84	14.72	14.51	9.42	19.13
S	27.68	27.82	24.71	26.03	27.29	27.12	27.88	26.53	28.38
Ag	0.17	0.23	0.46	0.19	0.09	0.47	n.d.	0.20	n.d.
Cu	41.49	41.44	39.05	39.49	40.49	39.76	43.97	40.19	43.45
Ni	n.d.	n.d.	n.d.	n.d.	n.d.	n.d.	n.d.	n.d.	n.d.
Ge	n.d.	n.d.	n.d.	n.d.	n.d.	n.d.	n.d.	n.d.	n.d.
Pb	0.06	n.d.	0.07	0.05	n.d.	0.07	n.d.	0.26	0.14
Sn	0.06	0.05	0.04	0.08	n.d.	n.d.	n.d.	n.d.	n.d.
Fe	3.46	3.42	2.40	2.18	2.17	0.31	4.70	2.09	3.21
Zn	2.11	2.20	3.42	4.43	5.09	6.26	0.67	5.65	4.38
Se	n.d.	n.d.	0.03	0.07	0.02	0.03	n.d.	0.06	0.05
Sb	18.21	20.14	16.17	20.03	15.08	11.08	8.80	15.88	0.16
In	0.08	0.05	0.07	0.08	0.07	0.05	n.d.	n.d.	n.d.
Co	0.02	0.02	0.03	0.04	0.03	0.08	0.19	0.19	n.d.
Te	n.d.	n.d.	n.d.	n.d.	n.d.	n.d.	n.d.	n.d.	n.d.
Au	0.02	n.d.	0.11	0.01	n.d.	0.05	n.d.	n.d.	n.d.
Cd	0.05	0.02	0.08	0.16	n.d.	0.02	n.d.	0.08	0.10
Bi	0.11	0.02	0.16	0.05	0.19	0.17	n.d.	n.d.	2.01
Hg	0.12	0.15	3.72	0.35	0.45	0.41	n.d.	n.d.	0.09
Mo	0.04	0.01	0.05	0.06	0.06	n.d.	0.05	n.d.	0.13
Mn	n.d.	n.d.	n.d.	n.d.	n.d.	n.d.	n.d.	n.d.	n.d.
∑ wt%	100.98	101.76	98.91	99.57	100.86	100.60	100.88	100.64	101.48
As	1.459	1.236	1.878	1.336	2.002	3.013	2.890	1.972	3.743
S	13.000	13.000	12.994	12.986	12.996	12.994	13.000	13.000	13.000
Ag	0.024	0.032	0.072	0.029	0.013	0.067	n.d.	0.029	n.d.
Cu	9.814	9.753	10.342	9.923	9.712	9.595	10.326	9.919	10.025
Ni	n.d.	n.d.	n.d.	n.d.	n.d.	n.d.	n.d.	n.d.	n.d.
Ge	n.d.	n.d.	n.d.	n.d.	n.d.	n.d.	n.d.	n.d.	n.d.
Pb	0.004	n.d.	0.006	0.004	n.d.	0.005	n.d.	0.020	0.010
Sn	0.008	0.006	0.006	0.011	n.d.	n.d.	n.d.	n.d.	n.d.
Fe	0.931	0.916	0.723	0.623	0.592	0.085	1.256	0.587	0.843
Zn	0.485	0.503	0.880	1.082	1.186	1.468	0.153	1.355	0.982
Se	n.d.	n.d.	0.006	0.014	0.004	0.006	n.d.	0.012	0.010
Sb	2.248	2.474	2.235	2.627	1.888	1.396	1.079	2.046	0.019
In	0.010	0.006	0.010	0.012	0.009	0.007	n.d.	n.d.	n.d.
Co	0.004	0.005	0.009	0.010	0.008	0.021	0.047	0.049	n.d.
Te	n.d.	n.d.	n.d.	n.d.	n.d.	n.d.	n.d.	n.d.	n.d.
Au	0.002	<0.001	0.009	<0.001	n.d.	0.004	n.d.	n.d.	n.d.
Cd	0.007	0.002	0.012	0.022	n.d.	0.003	n.d.	0.011	0.013
Bi	0.008	0.002	0.013	0.004	0.014	0.012	n.d.	n.d.	0.141
Hg	0.009	0.011	0.312	0.028	0.034	0.031	n.d.	n.d.	0.007
Mo	0.006	0.001	0.009	0.010	0.009	n.d.	0.008	n.d.	0.020
Mn	n.d.	n.d.	n.d.	n.d.	n.d.	n.d.	n.d.	n.d.	n.d.
Sb/As	1.541	2.002	1.190	1.966	0.943	0.463	0.373	1.038	0.005
∑Me	11.292	11.229	12.370	11.710	11.519	11.275	11.790	11.970	11.900
Fe+Zn	1.416	1.419	1.604	1.705	1.779	1.553	1.409	1.942	1.825
XAs	0.393	0.333	0.455	0.337	0.513	0.682	0.728	0.491	0.959
XSb	0.605	0.667	0.542	0.662	0.484	0.316	0.272	0.509	0.005
XBi	0.002	n.d.	0.003	0.001	0.004	0.003	n.d.	n.d.	0.036

Mineral formulae of all fahlore-group minerals were calculated on the basis of 13 S + Se. X_{Sb} = Sb/(Sb + As + Te + In + Bi + Ge); X_{As} = As/(Sb + As + Te + In + Bi + Ge); X_{Bi} = Bi/(Sb + As + Te + In + Bi + Ge); n.d.: not detected.

Tab. 2a: Representative electron-probe microanalyses of fahlore-group minerals

	Röhrerbühel			Pfunderer Berg		
As	7.62	4.43	2.42	0.69	1.84	0.44
S	25.38	25.19	24.79	23.94	24.72	24.84
Ag	0.31	0.97	0.37	10.50	7.27	3.12
Cu	39.78	38.32	39.09	30.08	32.34	36.38
Ni	n.d.	0.02	n.d.	n.d.	n.d.	0.01
Ge	n.d.	n.d.	n.d.	n.d.	n.d.	0.01
Pb	0.10	n.d.	n.d.	n.d.	0.15	0.12
Sn	n.d.	0.06	0.12	n.d.	n.d.	n.d.
Fe	5.99	6.33	5.72	3.48	1.18	3.17
Zn	1.36	1.70	2.04	3.58	7.43	4.18
Se	0.01	n.d.	0.04	n.d.	0.03	n.d.
Sb	18.34	23.17	25.28	27.91	26.32	28.58
In	0.10	0.07	0.10	0.08	0.10	0.07
Co	0.04	n.d.	0.03	n.d.	n.d.	n.d.
Te	n.d.	n.d.	n.d.	n.d.	n.d.	n.d.
Au	0.06	0.02	0.06	0.03	n.d.	0.03
Cd	0.02	0.02	0.07	0.16	0.15	0.13
Bi	0.07	0.02	0.10	n.d.	0.05	0.03
Hg	0.07	0.04	0.05	0.03	n.d.	n.d.
Mo	0.08	0.03	0.03	0.13	0.03	0.01
Mn	n.d.	0.01	n.d.	n.d.	n.d.	n.d.
∑ wt%	99.32	100.41	100.30	100.60	101.61	101.13
As	1.667	0.977	0.542	0.160	0.413	0.099
S	12.998	13.000	12.992	13.000	12.993	13.000
Ag	0.046	0.148	0.058	1.692	1.134	0.484
Cu	10.261	9.961	10.318	8.227	8.561	9.590
Ni	n.d.	0.005	n.d.	n.d.	n.d.	0.003
Ge	n.d.	n.d.	n.d.	n.d.	0.001	0.003
Pb	0.008	n.d.	n.d.	n.d.	0.012	0.010
Sn	n.d.	0.008	0.017	n.d.	n.d.	n.d.
Fe	1.758	1.872	1.718	1.083	0.355	0.951
Zn	0.341	0.429	0.523	0.952	1.911	1.071
Se	0.002	n.d.	0.008	n.d.	0.007	n.d.
Sb	2.469	3.143	3.483	3.984	3.637	3.932
In	0.014	0.010	0.014	0.012	0.014	0.010
Co	0.012	n.d.	0.007	n.d.	n.d.	n.d.
Te	n.d.	n.d.	n.d.	n.d.	n.d.	n.d.
Au	0.005	0.002	0.005	0.003	n.d.	0.002
Cd	0.003	0.004	0.010	0.024	0.022	0.020
Bi	0.005	0.002	0.008	n.d.	0.004	0.003
Hg	0.005	0.003	0.004	0.002	n.d.	n.d.
Mo	0.013	0.004	0.006	0.023	0.005	0.002
Mn	n.d.	0.003	n.d.	n.d.	n.d.	n.d.
Sb/As	1.481	3.217	6.426	24.927	8.803	39.881
∑Me	12.447	12.435	12.661	12.002	12.002	12.130
Fe+Zn	2.099	2.301	2.241	2.035	2.267	2.022
XAs	0.403	0.237	0.134	0.039	0.102	0.024
XSb	0.596	0.762	0.864	0.961	0.897	0.975
XBi	0.001	n.d.	0.002	n.d.	0.001	0.001

Mineral formulae of all fahlore-group minerals were calculated on the basis of 13 S + Se. X_{Sb} = Sb/(Sb + As + Te + In + Bi + Ge); X_{As} = As/(Sb + As + Te + In + Bi + Ge); X_{Bi} = Bi/(Sb + As + Te + In + Bi + Ge); n.d.: not detected.

Tab. 2b: Representative electron-probe microanalyses of fahlore-group minerals

	Bartholomäberg			Mitterberg		
As	3.05	1.74	5.66	4.01	17.86	11.42
S	24.77	25.25	25.33	25.22	30.14	27.70
Ag	0.74	0.53	0.44	0.01	0.05	0.13
Cu	37.25	37.47	37.57	36.22	41.45	40.03
Ni	0.01	n.d.	n.d.	2.12	0.02	0.01
Ge	n.d.	n.d.	n.d.	n.d.	n.d.	n.d.
Pb	0.05	0.02	0.12	0.02	0.08	0.11
Sn	0.07	0.12	0.06	0..37	0.19	0.04
Fe	5.13	5.02	6.73	6.26	7.19	5.26
Zn	2.20	2.19	2.41	0.34	0.29	2.77
Se	0.02	n.d.	0.01	n.d.	n.d.	0.03
Sb	24.55	26.58	21.13	26.30	1.70	13.02
In	0.05	0.10	0.05	0.08	0.12	n.d.
Co	n.d.	0.03	0.01	0.06	0.01	0.01
Te	n.d.	n.d.	n.d.	n.d.	n.d.	n.d.
Au	0.10	n.d.	0.03	n.d.	0.03	n.d.
Cd	0.10	n.d.	0.12	0.13	0.02	n.d.
Bi	0.84	0.87	0.65	0.54	0.05	0.05
Hg	0.41	0.25	0.18	0.36	0.15	0.32
Mo	0.02	0.06	0.07	n.d.	0.02	0.08
Mn	n.d.	n.d.	n.d.	n.d.	n.d.	n.d.
∑ wt%	99.35	100.24	100.66	101.35	99.38	100.98
As	0.684	0.383	1.241	0.663	3.291	2.289
S	13.000	13.000	13.000	13.000	13.000	12.995
Ag	0.115	0.081	0.067	0.002	0.006	0.018
Cu	9.847	9.716	9.712	9.404	9.005	9.459
Ni	0.003	n.d.	n.d.	0.596	0.004	0.003
Ge	n.d.	n.d.	n.d.	n.d.	n.d.	n.d.
Pb	0.004	0.002	0.010	0.002	0.005	0.008
Sn	0.010	0.017	0.008	0.051	0.023	0.005
Fe	1.543	1.481	1.979	1.849	1.777	1.414
Zn	0.565	0.552	0.605	0.086	0.062	0.636
Se	0.004	n.d.	0.004	n.d.	n.d.	0.005
Sb	3.387	3.597	2.851	3.564	0.193	1.606
In	0.007	0.014	0.007	0.011	0.015	n.d.
Co	n.d.	0.008	0.003	0.017	0.003	0.001
Te	n.d.	n.d.	n.d.	n.d.	n.d.	n.d.
Au	0.009	n.d.	0.003	n.d.	0.002	n.d.
Cd	0.015	n.d.	0.018	0.019	0.003	n.d.
Bi	0.068	0.069	0.051	0.043	0.003	0.004
Hg	0.034	0.021	0.015	0.030	0.010	0.024
Mo	0.004	0.010	0.012	n.d.	0.003	0.012
Mn	n.d.	n.d.	n.d.	n.d.	0.001	n.d.
Sb/As	4.953	9.402	2.297	5.376	0.059	0.702
∑Me	11.731	11.743	11.999	12.056	10.901	11.580
Fe+Zn	2.037	2.008	2.496	1.935	1.839	2.050
XAs	0.165	0.095	0.300	0.155	0.944	0.587
XSb	0.819	0.889	0.688	0.835	0.055	0.412
XBi	0.016	0.017	0.012	0.010	0.001	0.001

Mineral formulae of all fahlore-group minerals were calculated on the basis of 13 S + Se. X_{Sb} = Sb/(Sb + As + Te + In + Bi + Ge); X_{As} = As/(Sb + As + Te + In + Bi + Ge); X_{Bi} = Bi/(Sb + As + Te + In + Bi + Ge); n.d.: not detected.

Tab. 2c: Representative electron-probe microanalyses of fahlore-group minerals

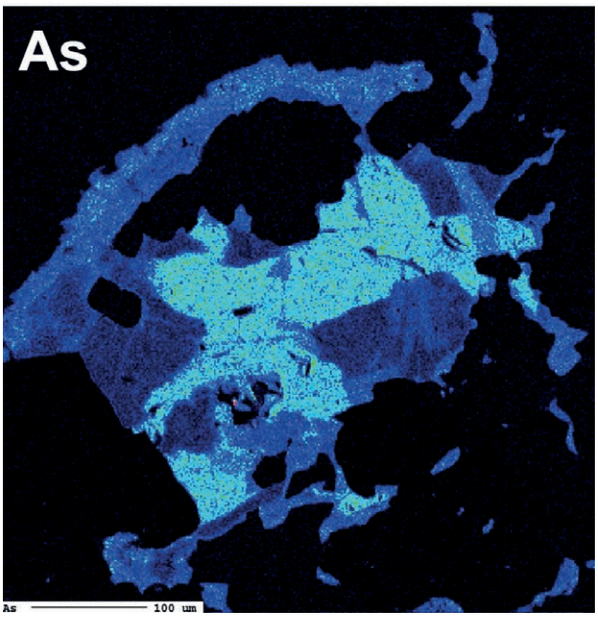

Fig. 5: Elemental distribution map of As of a complex zoned fahlore-group mineral from Bartholomäberg.

which corresponds to a freibergite mole fraction of 94.5%. The Ag concentrations show moderate variations, with a minimum freibergite mole fraction of 0.93% and a mean Ag concentration of 14.89 wt.%. Their chemical composition is in contrast to that of the large fahlore grains that are intergrown with chalcopyrite, sphalerite, pyrite and galena. The mean As concentration of the matrix fahlore is 0.96 wt.%, corresponding to 94.5% of the tetrahedrite end-member. The highest measured tetrahedrite mole fraction is 99.25%. Another notable chemical feature of the fahlore inclusions is their high Cd concentrations. Even if measured Cd concentrations <1 wt.% can be attributed at least in part to analytical interferences with Ag, the maximum measured value of 11.2 wt.% indicates uncommonly high Cd concentrations. Some analyses show Au concentrations up to 0.09 wt%. Chemical analyses of fahlore-group minerals are listed in Table 2b.

Bartholomäberg-Silbertal

The fahlore-group minerals show extensive As-Sb substitution on the X-site, between 0.029 a.p.f.u. As and 3.967 a.p.f.u. Sb (close to end-member tetrahedrite) and 2.602 a.p.f.u. As and 1.279 a.p.f.u. Sb (tennantite-tetrahedrite solid solution). The mean Fe and Zn contents are 1.532 and 0.508 a.p.f.u., respectively. In addition, minor amounts of In (average 0.012 a.p.f.u.), Bi (0.048 a.p.f.u.), Hg (0.024 a.p.f.u.) and Ag (0.070 a.p.f.u.) occur. Hg concentrations vary between 0.007 and 0.046 a.p.f.u. Hg and Ag concentrations vary between 0.049 and 0.111 a.p.f.u. Fahlore-group mineral analyses from the Kristbergsattel show on average 1.783 a.p.f.u. As and 2.108 a.p.f.u. Sb. The concentrations of Ag, In, Hg, Bi are similar to Bartholomäberg but Zn varies from 0.323 to 1.551 a.p.f.u. Zn (mean 0.561 a.p.f.u.). Representative analyses from Bartholomäberg are given in Table 2c.

Mitterberg

Elemental concentrations of the fahlore-group minerals show extensive As-Sb substitution on the X-site, with As in the range 0.663-3.298 a.p.f.u. and Sb in the range 0.193-3.673 a.p.f.u. Concentrations of Zn and Fe on the M(1)-site range from 0.017 a.p.f.u. to 0.382 a.p.f.u. and from 1.262 a.p.f.u. to 1.876 a.p.f.u., respectively (Table 2c). In addition small concentrations of Ni, Se, Bi, Hg and Sn could be detected.

Discussion

The complex geological evolution of the Alpine ore deposits

The Alpine-Balkan-Carpathian-Dinaride belt is one of the world's oldest mining areas and played a major role in the history of European civilization, from the prehistory up until the present day (Heinrich & Neubauer, 2002). This metallogenic and geodynamic province is part of the Alpine-Himalayan orogenic system, which is the result of the convergence between the African, Arabian and Indian plates and Eurasia, which took place mainly from the Cretaceous to the present. As a result of the complex Paleozoic as well as Mesozoic and Paleogene geodynamic history, with several oceanic basins and continental microplates involved, the metallogeny of the Alpine-Balkan-Carpathian-Dinaride belt region involved several phases of major ore formation and subsequent ore re-mobilisation. Due to the geodynamic evolution circulation of metamorphic fluids plays an important role in the genesis of the ore deposits of the Eastern Alps. Metamorphic mineral deposits are thought to have formed from hydrothermal solutions, which are expelled from geological bodies undergoing prograde metamorphism (Hanson, 1997). This may either be prograde, and then the fluids are predominantly the product of de-volatilization, or metamorphism may be retrograde, in which case the water involved can have various sources (marine, meteoric, etc.). Accordingly, specific deposits may have been formed by mixing of ascending devolatilization fluids with convecting meteoric waters. Tectonic control of these mineralizations is late-orogenic trans-tensional faulting, which exposed hot metamorphic rocks to fluid convection along brittle structures. All the ore deposits considered in this study record an early stage of mineral deposition during the Paleozoic, but many of them experienced extensive re-mobilisation under low temperatures mainly during the Eo-Alpine/Alpine orogeny (Neubauer

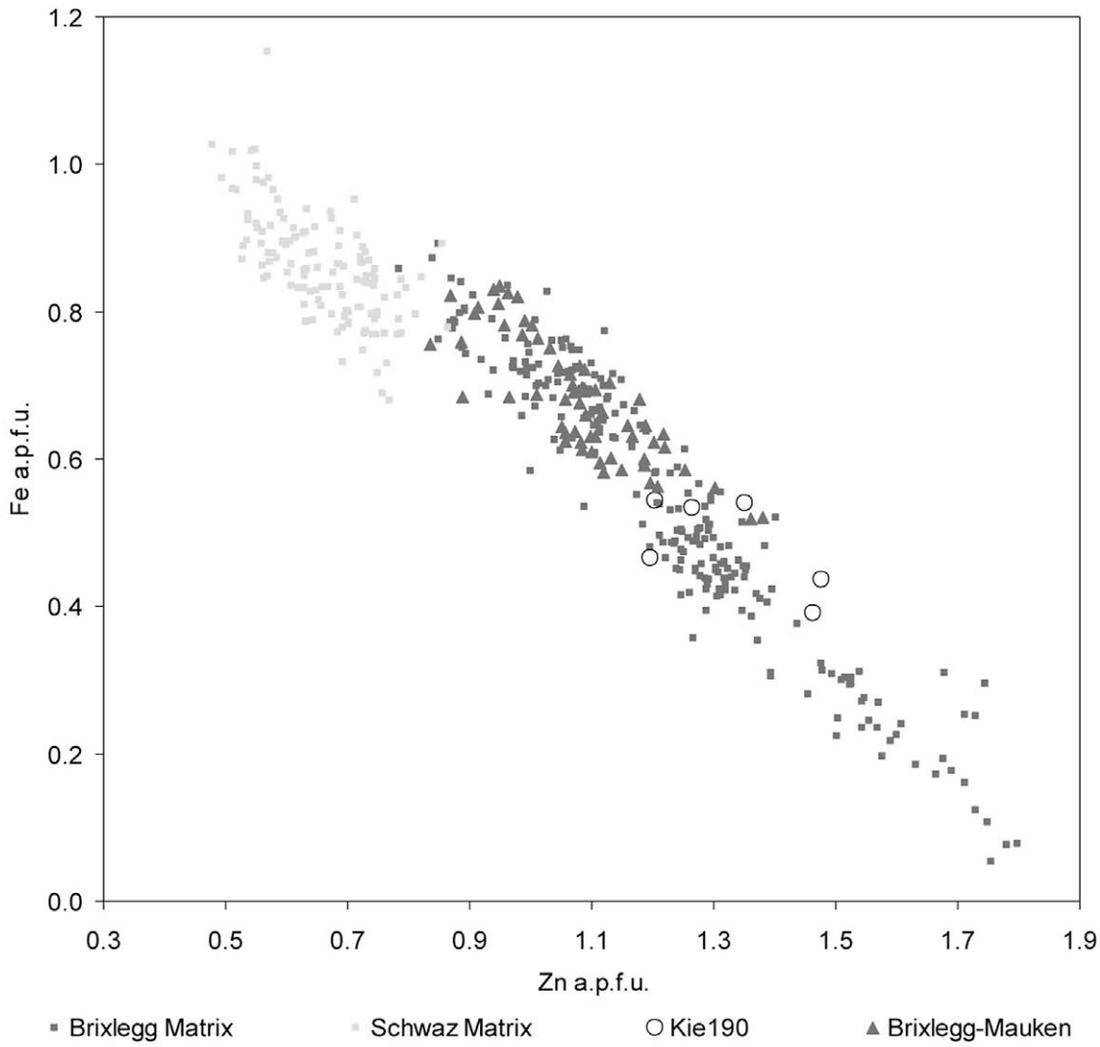

Fig. 6: Plot of Fe vs Zn of the fahlore-group minerals from Schwaz (light grey squares), Brixlegg (dark squares), Brixlegg-Mauken (dark grey triangles) and from an ore fragment in a slag fragment (Kie 190) from the Kiechlberg (open circles).

& Heinrich, 2003). This is evident in many ore textures showing complex chemical zoning patterns involving veining textures in fahlore-group minerals (Fig. 5, As zoning in fahlore-group minerals from Bartholomäberg) and the geothermometric estimates. Temperatures obtained by fluid inclusion microthermometry (Bechter, 2009) or siderite-ankerite geothermometry (Viertler, 2011) yielded temperatures ranging from <100°C up to 300°C some of the ore deposits investigated in this study. Among the ore deposits studied here, the only high-temperature ore deposit is the Pfunderer Berg ore deposit, which yields temperatures >500°C, consistent with its direct genetic link with the intrusion of small diorite bodies during the Permian (Krismer et al., 2011b). Keeping in mind the observations in Figure 5, the complex chemical zoning patterns of the main ore minerals has to be considered with caution when using mineral chemical data for ore provenance studies.

The prehistoric ore deposit – mining connection

The comparison between the ore mineral assemblage of prehistorically mined ore deposits in the Eastern- and Southern Alps clearly shows that here chalcopyrite and fahlore-group minerals were the most important phases used for the prehistoric copper production (Weisgerber & Goldenberg, 2004; Lutz & Pernicka, 2013; Pernicka & Lutz, 2015; Artioli et al., 2016). The beginning of Cu-metallurgy in the Eastern- and Southern Alps can be set into the Late Neolithic to Early Bronze Age. The earliest evidence of smelting and copper production in the Eastern Alps is known from the Mariahilfbergl near Brixlegg, which is located in the vicinity of the fahlore deposits of Brixlegg. Here the copper slags are associated with ceramics from the Münchshöfener culture, dating to the beginning of the Late Neolithic in southern Germany

(4500 - 4000 BC) (Bartelheim et al., 2002; Höppner et al., 2005). Early Bronze Age metallurgy has also been reported from the Buchberg near Wiesing in the Lower Inn Valley (Martinek, 1996; Martinek and Sydow, 2004). In the Middle- and Late Bronze Age abundant Cu metallurgy in the central Eastern and Southern Alps is known from the Mitterberg mining district (Salzburg, Austria) (Stöllner et al., 2004; 2006) from the Kelchalm/Jochberg/Kitzbühel mining district (North Tyrol, Austria) (Goldenberg, 2004) and from the Schwaz-Brixlegg mining district (North Tyrol, Austria) (Goldenberg & Rieser, 2004; Krismer et al., 2010; Goldenberg, 2015). In the Southalpine namely in the Trentino and Alto Adige/ South Tyrol regions, there is substantial evidence of Copper Age (e.g. Artioli et al., 2015) and Bronze Age (Metten, 2003; Cierny et al., 2004; Cierny, 2008; Addis et al., 2016, 2017) smelting activities. With regard to the temporal use of Cu-ores investigations of Lutz and Pernicka (2013) and Pernicka and Lutz (2015) show that at the beginning of the Early Bronze Age the fahlore copper of the Inn Valley dominates the region. In the Middle Bronze Age it is replaced by the east Alpine copper of the Mitterberg type. Fahlore copper reappears in the Late Bronze Age and is used parallel to east Alpine copper. In this period mixing of chalcopyrite and fahlore copper is also common.

In the Austroalpine Mitterberg and Kelchalm/Jochberg/Kitzbühel mining districts chalcopyrite is the predominant Cu carrier (Stöllner et al., 2004, 2006; Goldenberg, 2004). Concerning the Southalpine mining districts Pfunderer Berg (South-Tyrol) and various sites from the Trentino chalcopyrite is also the most dominant Cu carrier (Metten, 2003; Nimis et al., 2012; Artioli et al., 2016; Addis et al., 2017). Contrary the smelting sites from the North Tyrolean Lower Inn Valley provide evidence for the processing of fahlore-group minerals with dominantly tetrahedrite-tennantite composition (Krismer et al., 2012; Goldenberg, 2015). This resulted in elevated Zn concentrations, the presence of Ag (e.g. from fahlore-group minerals and/or balkanite in Röhrerbühel) and in some cases traces of Co and Ni (e.g. from Co-Ni bearing tetrahedrite-tennantite) in the smelting products. Different elemental distributions hance can be expected from the Southalpine smelting sites. The sphalerite- and galena-rich veins that accompany the chalcopyrite-rich vein at Pfunderer Berg were probably only of minor interest in prehistoric times, but the chalcopyrite-rich domains most likely were of considerable interest since Eneolithic times (Artioli et al., 2015). Since the chalcopyrite-rich domains contain sphalerite, galena, pyrite and Ag-bearing phases, this would produce slags and raw metals with elevated Zn, Fe, Pb and Ag contents during smelting, unless chalcopyrite was efficiently pre-concentrated before smelting. Due to the presence of Bi-phases elevated Bi concentrations in metallurgical products (especially in metal and sulfide phases) may also be expected. During smelting Fe and Zn would form silicates such as Zn-bearing fayalite, Zn-bearing clinopyroxene and Zn-bearing åkermanite/gehlenite and Ag and Pb would remain similar to Bi predominantly in the obtained metal or within distinct sulfide enclaves of the slags and the raw metal. Therefore the chemical major-, minor- and trace element contents of Southalpine metallurgical products will show a different geochemical signature and thus can be probably distinguished from the products of ores from the North Tyrolean and Salzburg sites in the Greywacke Zone (Artioli et al., 2016).

Linking smelting site and ore deposit - the example of the Kiechlberg

The Kiechlberg is a small hill at 1028 metres above sea level on the southern side of the Karwendel mountain range, a few kilometers northeast of Innsbruck. Superficial finds of artefacts and metallurgical slags led to first archaeological excavations, which started in 2007 in the frame of the SFB HiMAT (Töchterle, 2015). On the Kiechlberg, a huge amount of ceramic and flint artefacts as well as some metal objects made of copper and bronze were collected during the investigation of different prehistoric waste layers, indicating an occupation of the site from the Late Neolithic up to the Middle Bronze Age. Together with archaeological finds and almost in the upper layers of the studied stratigraphy, various slags and copper-rich semiproducts (unrefined antimony-rich raw copper) occur and prove primary copper metallurgy at the site during the Early Bronze Age. Unfortunately, no direct evidence of smelting facilities could be excavated at the Kiechlberg site. Many of the slag samples occur only as small fragments without any archaeological or macroscopic evidence whether they have been produced in a furnace, hearth or crucible or cooled in a separate receptacle (Hauptmann et al., 2003). It is suggested for this period that the charge was smelted with the aid of blowpipes and clay tuyeres within a crucible in a small hearth structure (shallow pit, Töchterle et al., 2013). The mineralogy of the excavated copper ore fragments (fahlore-group minerals with enargite-famatinite mineral reaction domains) as well as the chemical composition of slags and raw metal remains suggest that the smelted ore was primarily fahlore-group minerals mixed with enargite-famatinite, malachite, azurite and other secondary copper minerals (Cu-Zn-Sb-As oxides). The mineral assemblage as well as the chemical composition of the ore fragments from the Kiechlberg site match very well the ore mineralogy found in the mining district of Brixlegg/Radfeld including the Mauken area. Figure 6 shows the comparison of Fe/Zn ratios of EPMA spot analyses of fahlore-group minerals from an ore sample found at the Kiechlberg (Kie 190) and the Devonian dolomite-hosted fahlore-group minerals from Schwaz and Brixlegg. This diagram shows a very good agreement between the composition of the ore fragments from sample Kie 190 and the fahlore-group mineral compositions from Brixlegg (Krismer et al., 2011b). All these facts together suggest that the main sources of copper ores used for the copper production at the Kiechlberg site were the large fahlore-group mineral deposits of Brixlegg.

Acknowledgments

The financial support through the Austrian Science Fund FWF special research program HiMAT (F3110-G02) is gratefully acknowledged. Paolo Nimis is thanked for his thorough and concise review, which helped to clarify matters considerably. Rouven Turck is also thanked for his editorial handling of the manuscript.

Bibliography

Addis, A., Angelini, I. & Artioli, G., 2017. Late Bronze Age copper smelting in the southeastern Alps: how standardized was the smelting process? Evidence from Transacqua and Segonzano, Trentino, Italy. *Archaeological and Anthropological Sciences* 9, pp.985-999.

Addis, A., Angelini, I., Nimis, P. & Artioli, G., 2016. Late Bronze Age copper smelting slags from Luserna (Trentino, Italy): interpretation of the metallurgical process. *Archaeometry* 58, pp.96-114.

Arlt, T. & Diamond, L., 1998. Composition of tetrahedrite-tennantite and 'schwazite' in the Schwaz silver mines, North Tyrol, Austria. *Mineralogical Magazine* 62/6, pp.801-820.

Artioli, G., Angelini, I., Tecchiati, U. & Pedrotti, A., 2015. Eneolithic copper smelting slags in the Eastern Alps: Local patterns of metallurgical exploitation in the Copper Age. *Journal of Archaeological Science 63*, pp.78-83.

Artioli, G., Angelini, I., Nimis, P. & Villa, I. M., 2016. A lead-isotope database of copper ores from the Southeastern Alps: A tool for the investigation of prehistoric copper metallurgy. *Journal of Archaeological Science 75*, pp.27-39.

Bartelheim, M., Eckstein, K., Huijsmans, M., Krauss, R. & Pernicka, E., 2002. Kupferzeitliche Metallgewinnung in Brixlegg, Österreich. In: Bartelheim, M., Pernicka, E. & Krause, R. eds. *Die Anfänge der Metallurgie in der Alten Welt.* Rahden: Leidorf, pp.33-82.

Bechter, D., A., 2009. *Petrologische, geochemische und montanarchäologische Untersuchungen der historischen Kupferlagerstätte Bartholomäberg und Silbertal.* Unpublished M.Sc. *Thesis*, University of Innsbruck.

Brigo, L., 1971. Mineralizzazioni e metallogenesi nell'area della Fillade quarzifera di Bressanone nelle Alpi Sarentine. *Studi Trentini di Scienze Naturali* A48, pp.80-125.

Cesare, B., Mazzoli, C., Sassi, R., Spiess, R. & Sassi, F. P., 2010. Beauty and complexity of metamorphism: case studies from the frontal part of the Adria microplate. *Rendiconti Lincei 21*, pp.73-94.

Cierny, J., 2008. Prähistorische Kupferproduktion in den südlichen Alpen, Region Trentino Orientale. *Der Anschnitt*, Beiheft 22, Bochum.

Cierny, J., Marzatico, F., Perini, R. & Weisgerber, G., 2004. Der spätbronzezeitliche Verhüttungsplatz Acqua Fredda am Passo Redebus (Trentino). In: G. Weisgerber, & G. Goldenberg, eds. *Alpenkupfer Rame delle Alpi,* Der Anschnitt Beiheft 17, Bochum: Deutsches Bergbau-Museum, pp.155-164.

Dorfmann, W., 1974. *Le miniere nella zona di Chiusa (Der Bergbau im Raume Klausen).* Unpublished Dissertation, University of Padua, Padua.

Ebner, F. & Weber, L., 1997. *Die geologischen Einheiten Österreichs und ihre Rohstoffe. Metallogenetische Karte von Österreich (1: 500.000) und Handbuch der Lagerstätten der Erze, Industrieminerale und Energierohstoffe Österreichs.* Archiv für Lagerstättenforschung der Geologischen Bundesanstalt (Austria) *19*, pp.49-229.

Exel, R., 1998. *Lagerstättenkundliche und montanhistorische Erhebungen über den Erzbergbau in Südtirol (Provinz Bozen, Italien).* Berichte der Geologischen Bundesanstalt (Austria) 42.

Frimmel, H.E., 1991. Isotopic constrains on fluid/rock ratios in carbonate rocks: Barite-sulfide mineralizations in the Schwaz Dolomite, Tyrol (Eastern Alps, Austria). *Chemical Geology* 90, pp.195-209.

Frimmel, H. E. & Papesch, W., 1990. Sr, O and C Isotope Study of the Brixlegg Barite Deposit, Tyrol (Austria). *Economic Geology* 85, pp.1162-1171.

Fuchs, H. W., 1988. Die transversalen Erzgänge im Gefolge der herzynischen Granitintrusionen in Südtirol. L. Weber, ed. *Handbuch der Lagerstätten der Erze, Industrieminerale und Energierohstoffe Österreichs.* Archiv für Lagerstättenforschung der Geologischen Bundesanstalt (Austria) 19, pp.19-32.

Gisser, A., 1926. Zur Petrographie der Klausenite. Verlag Wagner, Innsbruck.

Goldenberg, G. & Rieser, B., 2004. Die Fahlerzlagerstätten von Schwaz/Brixlegg (Nordtirol) – Ein weiteres Zentrum urgeschichtlicher Kupferproduktion in den österreichischen Alpen. In: G. Weisgerber, & G. Goldenberg, eds. *Alpenkupfer Rame delle Alpi,* Der Anschnitt Beiheft 17, Bochum: Deutsches Bergbau-Museum, pp.37-53.

Goldenberg, G., 2015. Prähistorische Kupfergewinnung aus Fahlerzen der Lagerstätte Schwaz-Brixlegg im Unterinntal, Nordtirol. In: Th. Stöllner & K. Oeggl, eds. *Bergauf Bergab. 10000 Jahre Bergbau in den Ostalpen. Wissenschaftlicher Beiband zur Ausstellung Bochum und Bregenz*. Veröffentlichungen DBM 207, Bochum-Rahden: Deutsches Bergbau-Museum Bochum in Kommission bei Marie Leidorf, pp.151-163.

Goldenberg, G., 2004. Ein Verhüttungsplatz der mittleren Bronzezeit bei Jochberg. In: G. Weisgerber, & G. Goldenberg, eds. *Alpenkupfer Rame delle Alpi,* Der Anschnitt Beiheft 17, Bochum: Deutsches Bergbau-Museum, pp.165-176.

Gstrein, P., 1979. Neuerkenntnisse über die Genese der Fahlerzlagerstätte Schwaz (Tirol). *Mineralium Deposita* 14, pp.185-194.

Haditsch, J.G. & Mostler, H., 1986. Jungalpidische Kupfervererzungen im Montafon (Vorarlberg). *Geologisch Paläontologische Mitteilungen der Universität Innsbruck* 13, pp.277-296.

Hanson, R.B., 1997. Hydrodynamics of regional metamorphism due to continental collison. *Economic Geology* 92, pp.880-891.

Heinisch, H., 1988. Hinweise auf die Existenz eines passiven Kontinetalrandes im Altpaläozoikum der Nördlichen Grauwackenzone-Ostalpen. *Schweizerische Mineralogische und Petrographische Mitteilungen* 68, pp.407-418.

Heinrich, C.A. & Neubauer, F., 2002. Cu-Au-Pb-Zn-Ag metallogeny of the Alpine-Balkan-Carpathian-Dinaride geodynamic province. *Mineralium Deposita* 37, pp.533-540.

Hauptmann, A., Rehren, Th. & Schmitt-Strecker, S., 2003. Early Bronze Age copper metallurgy at Shahr-i Sokhta (Iran), reconsidered. In: Th. Stöllner, G. Körlin, G. Steffens. & Cierny J. eds. *Man and Mining – Mensch und Bergbau.* Der Anschnitt, Beiheft 16, Bochum: Deutsches Bergbau-Museum, pp.197-213.

Hoinkes, G., Koller, F., Rantitsch, G., Dachs, E., Höck, V., Neubauer, F. & Schuster, R., 1999. Alpine metamorphism of the Eastern Alps. *Schweizerische Mineralogische und Petrographische Mitteilungen* 79, pp.155-181.

Höppner, B., Bartelheim, M., Huijsmans, M., Krauss, R., Martinek, K.-P., Pernicka, E. & Schwab, R., 2005. Prehistoric copper production in the Inn Valley (Austria), and the earliest copper in central Europe. *Archaeometry* 47, pp.293-315.

Johnson, N. E., Craig, J. R. & Rimstidt, J. D., 1988. Crystal chemistry of tetrahedrite. *American Mineralogist* 73, pp.389-397.

Junghans, S., Sangmeister, E. E. & Schröder, M., 1960. *Metallanalysen kupferzeitlicher und frühbronzezeitlicher Bodenfunde aus Europa.* Studien zu den Anfängen der Metallurgie I, Berlin.

Kharbish, S., Götzinger, M. & Beran, A., 2007. Compositional variations of fahlore group minerals from Austria. *Austrian Journal of Earth Sciences* 100, pp.44-52.

Krismer, M., Töchterle, U., Goldenberg, G., Vavtar, F., Tropper, P., Lutz, J. and Pernicka, E., 2010. A Mineralogical and Petrological Investigation of Early Bronze-Age Copper Slags from the Kiechlberg (North Tyrol, Austria). In: Anreiter, P., Goldenberg, G., Hanke, K., Krause, R., Leitner, W., Mathis, M., Nicolussi, K., Oeggl, K., Pernicka, E., Prast, M., Schibler, J., Schneider, I., Stadler, H., Stöllner, T., Tomedi, G., Tropper, P., eds*. Mining in European History and its Impact on Environment and Human Societies*. *Proceedings for the 1st Mining in European History-Conference of the SFB-HiMAT,* 12.-15. November 2009, Innsbruck: University Press, pp.107-109.

Krismer, M., Vavtar, F., Tropper, P., Kaindl, P. & Sartory, B., 2011a. Mineralogy and Petrology of Fahlore Breakdown in the Cu-Deposits Schwaz and Brixlegg (North Tyrol, Austria). *European Journal of Mineralogy* 23/6, pp.925-936.

Krismer, M., Vavtar, F., Tropper, P., Sartory, B. & Kaindl, R., 2011b. Mineralogy, mineral chemistry and petrology of the Ag-bearing Cu-Fe-Pb-Zn sulfide mineralizations of the Pfunderer Berg (South Tyrol, Italy). *Austrian Journal of Earth Sciences* 104/1, pp.36-48.

Krismer, M., Töchterle, U., Goldenberg, G., Tropper, P. & Vavtar, F., 2012. Mineralogical and petrological investigations of Early-Bronze age copper smelting remains from the Kiechlberg (Tyrol, Austria). *Archaeometry* 55, pp.923-945.

Lusk, J. & Calder B.O.E., 2004. The composition of sphalerite and associated sulfides in reactions of the Cu-Fe-Zn-S, Fe-Zn-S and Cu-Fe-S systems at 1 bar and temperatures between 250 and 535°C. *Chemical Geology* 203, pp.319-345.

Lutz, J. & Pernicka, E., 2013. Prehistoric copper from the Eastern Alps. *Open Journal of Archaeometry* 1, pp.122-127.

Martinek, K.-P., 1996. Archäometallurgische Untersuchungen zur frühbronzezeitlichen Kupferproduktion und -verarbeitung auf dem Buchberg bei Wiesing, Tirol. *Fundberichte aus Österreich* 34, pp.575-584.

Martinek, K.-P. & Sydow, W., 2004. Frühbronzezeitliche Kupfermetallurgie im Unterinntal (Nordtirol). In: G. Weisgerber, & G. Goldenberg, eds. *Alpenkupfer Rame delle Alpi,* Der Anschnitt Beiheft 17, Bochum: Deutsches Bergbau-Museum, pp.199-211.

Merwin, H.E., & Lombard, R.H., 1937. The system Cu-Fe-S. *Economic Geology 32*/2 Suppl., pp.203-284.

Metten, B., 2003. Beitrag zur spätbronzezeitlichen Kupfermetallurgie in Trentino (Südalpen) im Vergleich mit anderen prähistorischen Kupferschlacken aus dem Alpenraum. *Metalla* 10/1-2, pp.1-122.

Moh, G.H., 1975. Phase relations and mineral assemblages in the Cu-Fe-Zn-Sn-S system. *Chemie der Erde* 34, pp.1-61.

Mostler, H., 1970. Struktureller Wandel und Ursachen der Faziesdifferenzierung an der Ordoviz/Silur-Grenze in der Nördlichen Grauwackenzone (Österreich). *Festband des Geologischen Instituts der Universität Innsbruck 1970*, pp.507-522.

Mozgova, N.N., Tsepin, A.I. & Ozerova, N.A., 1980. Arsenic Schwazite. *Doklady Akadémii Nauk USSR, Earth Sciences Section* 239, pp.143-146.

Mutschlechner, G., 1968. Das Kitzbüheler Bergbaugebiet. *Stadtbuch Kitzbühel 2*, pp.11-30.

Neubauer, F., Hoinkes, G., Sassi, F. P., Handler, R., Höck, V., Koller, F. & Frank, W., 1999. Pre-Alpine metamorphism in the Eastern Alps. *Schweizerische Mineralogische und Petrographische Mitteilungen* 79, pp.41-62.

Neubauer, F., Heinrich, C. A. & Geode ABCD Working Group., 2003. Late Cretaceous and Tertiary geodynamics and ore deposit evolution of the Alpine-Balkan-Carpathian-Dinaride orogen. *Mineral exploration and sustainable development,* pp.1133-1136.

Niederschlag, E., Pernicka, E., Seifert, Th. & Bartelheim, M., 2003. Determination of Lead Isotope Ratios by Multiple Collector ICP-MS: A case study of Early Bronze Age Artefacts and their possible relation with ore deposits of the Erzgebirge. *Archaeometry* 45, pp.61-100.

Nimis, P., Omenetto, P., Giunti, I., Artioli, G., & Angelini, I., 2012. Lead isotope systematics in hydrothermal sulphide deposits from the central-eastern Southalpine (northern Italy). *European Journal of Mineralogy* 24, pp.23-37.

Oberhänsli, R., Bousquet, R., Engi, M., Goffé, B., Gosso, G., Handy, M., Koller, F., Lardeaux, J.-M., Polino, R., Rossi, P., Schuster, R., Schwartz, S., Spalla, I. E., Agard, P., Babist, J., Berger, A., Bertle, R., Bucher, K., Burri, T., Heitzmann, P., Hoinkes, G., Jolivet, L., Keller, L., Linner, M., Lombardo, B., Martinotti, G., Michard, A., Pestal, G., Proyer, A., Rantisch, G., Rosenberg, C., Schramm, J., Sölva, H., Thoeni, M., Zucali, M., 2004. *Metamorphic structure of the Alps 1:1000000.* Paris, CGMW.

Oberhauser, R., Rataj, W. & Geologische Bundesanstalt, 1998. *Geologisch-tektonische Übersichtskarte von Vorarlberg 1: 200000.* Wien: Geologische Bundesanstalt.

Panwitz, C., 2006. *Provenienzanalysen an paläozoischen Metasedimenten der Ostalpen mit Schwerpunkt der Nördlichen Grauwackenzone. Petrographie, Glimmerchemie, Ar-Ar Datierung.* Unpublished Ph.D Thesis, Halle-Wittenberg.

Pernicka, E. & Lutz, J., 2015: Fahlerz- und Kupferkies in der Bronze- und Eisenzeit. In: Th. Stöllner & K. Oeggl, eds. *Bergauf Bergab. 10000 Jahre Bergbau in den Ostalpen. Wissenschaftlicher Beiband zur Ausstellung Bochum und Bregenz.* Veröffentlichungen DBM 207, Bochum-Rahden: Deutsches Bergbau-Museum Bochum in Kommission bei Marie Leidorf, pp.107-111.

Piber, A., 2005. *The metamorphic evolution of the Austroalpine nappes north of the Tauern Window (Innsbruck Quartzphyllite Complex-Patscherkofel Crystalline Complex -Kellerjochgneiss and Wildschönau Schists).* Unpublished Ph.D. Thesis, Innsbruck.

Sack, R. O., 2017. Fahlore thermochemistry: Gaps inside the $(Cu,Ag)_{10}(Fe,Zn)_2(Sb,As)_4S_{13}$ cube. *Petrology 25*/5, pp.498-515.

Sassi, F. P. & Spiess, R., 1993. The Southalpine metamorphic basement in the Eastern Alps. In: J. F. Raumer, J.F. & F. Neubauer, eds. *The Pre-Mesozoic Geology in the Alps.* Berlin, pp. 599-607.

Schmid, S., Fügenschuh, B., Kissling, E. & Schuster, R., 2004. Tectonic map and overall architecture of the Alpine Orogen. *Eclogae Geologicae Helveticae, Swiss Journal of Geosciences* 97, pp.93-117.

Schulz, O., 1972. Unterdevonische Baryt-Fahlerz-Mineralisationen und ihre steilachsige Verformung im Grosskogel bei Brixlegg (Tirol). *Tschermaks Mineralogische und Petrographische Mitteilungen* 18, pp.114-128.

Schulz, O., 1997. Fahlerzbezirk Schwaz-Brixlegg und Kupfererzbezirk Röhrerbühel-Kitzbühel. L. Weber, ed. *Handbuch der Lagerstätten der Erze, Industriemineralien und Energierohstoffe Österreichs.* Archiv für Lagerstättenforschung der Geologischen Bundesanstalt (Austria) 19, pp.325-327.

Schulz, O. & Schroll, E., 1997. Pb-Zn-(Fahlerz-) Erzbezirk Anis Nordtiroler Kalkalpen. In: L. Weber, ed. *Handbuch der La-*

gerstätten der Erze, Industriemineralien und Energierohstoffe Österreichs. Archiv für Lagerstättenforschung der Geologischen Bundesanstalt (Austria) 19, pp.355-358.

Schuster, R., Koller, F., Höck, V., Hoinkes, G. & Bousquet, R., 2004. Explanatory notes to the map: metamorphic structure of the Alps, metamorphic evolution of the Eastern Alps. *Mitteilungen der Österreichischen Mineralogischen Gesellschaft* 149, pp.175-199.

Schuster, R., Scharbert, S., Abart, R. & Frank, W., 2001. Permo-Triassic extension and related HAT/LP metamorphism in the Austroalpine - Southalpine realm. *Mitteilungen der Gesellschaft der Geologie und Bergbaustudenten Österreichs* 45, pp.112-141.

Steiner, M., 2011. *Petrologie ausgewählter Cu-Lagerstätten (Kelchalm, Bachalm, Wildalm) im Revier Kitzbühel.* Unpublished Diploma Thesis, Innsbruck.

Steiner, M., Tropper, P., Vavtar, F. & Kaindl, R., 2010. Balkanite from the Cu ore deposit Röhrerbühel, Kitzbühel (N-Tyrol, Austria). *Neues Jahrbuch für Mineralogie* 187/2, pp.207-215.

Stöllner, Th., Eibner, C. & Cierny, J., 2004. Prähistorischer Kupferbergbau Arthurstollen – Ein neues Projekt im Südrevier des Mitterberg-Gebietes (Salzburg). In: In: G. Weisgerber, & G. Goldenberg, eds. *Alpenkupfer Rame delle Alpi,* Der Anschnitt Beiheft 17, Bochum: Deutsches Bergbau-Museum, pp.95-106.

Stöllner, T., Cierny, J., Eibner, C., Boenke, N., Herd, R., Maass, A., Röttger, K., Sormaz, T., Steffens, T. & Thomas, P., 2006. Der bronzezeitliche Bergbau im Südrevier des Mitterberggebietes. Bericht zu den Forschungen der Jahre 2002 bis 2006. *Archaeologia Austriaca* 90, pp.87-137.

Thöni, M., 1999. A review of geochronological data from the Eastern Alps. *Schweizerische Mineralogische und Petrographische Mitteilungen* 79, pp.209-230.

Töchterle, U., 2015. *Der Kiechlberg bei Thaur als Drehscheibe zwischen den Kulturen nördlich und südlich des Alpenhauptkammes. Ein Beitrag zum Spätneolithikum und zur Früh- und Mittelbronzezeit in Nordtirol.* Universitätsforschungen zur prähistorischen Archäologie 261, Bonn.

Töchterle, U., Goldenberg, G., Schneider, P. & Tropper, P., 2013. Spätbronzezeitliche Verhüttungsdüsen aus dem Bergbaurevier Mauken im Unterinntal, Nordtirol: Typologie, mineralogisch-petrographische Zusammensetzung und experimentelle Rekonstruktionsversuche. *Der Anschnitt* 65/1-2, pp.1-19.

Viertler, H.P., 2011. *Mineralogie und Petrologie von prähistorischen Kupferschlacken aus dem Gebiet Mitterberg.* Unpublished Diploma Thesis. Innsbruck.

Weber, L., 1997. Die metallogenetischen Einheiten Österreichs. In: L. Weber, ed. *Handbuch der Lagerstätten der Erze, Industriemineralien und Energierohstoffe Österreichs.* Archiv für Lagerstättenforschung der Geologischen Bundesanstalt (Austria) 19, pp.230-394.

Weidenbusch, H., 1849. Analyse des quecksilberhaltigen Fahlerzes von Schwatz in Tyrol. *Annalen der Physik und Chemie* 16, pp.86-88.

Weisgerber, G. & Goldenberg, G., eds. *Alpenkupfer Rame delle Alpi*. Der Anschnitt Beiheft 17, Bochum: Deutsches Bergbau-Museum.

Authors

Peter Tropper – Department of Mineralogy and Petrography, University of Innsbruck
Gert Goldenberg – Department of Archaeologies, University of Innsbruck
Matthias Krismer – Department of Mineralogy and Petrography, University of Innsbruck
Daniel Bechter – Department of Mineralogy and Petrography, University of Innsbruck
Martin Steiner – Department of Mineralogy and Petrography, University of Innsbruck
Hans-Peter Viertler – Department of Mineralogy and Petrography, University of Innsbruck
Franz Vavtar – Department of Mineralogy and Petrography, University of Innsbruck

Correspondence and material requests should be addressed to: Peter.Tropper@uibk.ac.at